Cellular Microbiology (2011) **13**(11), 1683–1702
doi:10.1111/j.1462-5822.2011.01647.x
First published online 24 August 2011

Lipid raft-dependent adhesion of *Giardia intestinalis* trophozoites to a cultured human enterocyte-like Caco-2/TC7 cell monolayer leads to cytoskeleton-dependent functional injuries

Martín A. Humen,[1,2,3] Pablo F. Pérez[3,4] and Vanessa Liévin-Le Moal[1,2,5]*

[1]*INSERM. UMR 756, 92296 Châtenay-Malabry. France.*
[2]*Université Paris-Sud 11, Faculté de Pharmacie. 92296 Châtenay-Malabry. France.*
[3]*Centro de Investigación y Desarrollo en Criotecnología de Alimentos. CCT-La Plata CIDCA-CONICET, Argentina.*
[4]*Cátedra de Microbiología. Departamento de Ciencias Biológicas. Facultad de Ciencias Exactas, Universidad Nacional de La Plata. 47 y 116-cc 553 1900 La Plata, Argentina.*
[5]*CNRS. UMR 8076 antiparasitaire », Faculté de Pharmacie, 92296 Châtenay-Malabry. France.*

Summary

***Gardia intestinalis*, the aetiological agent of giardiasis, one of the most common intestinal diseases in both developing and developed countries, induces a loss of epithelial barrier function and functional injuries of the enterocyte by mechanisms that remain unknown. Three possible mechanisms have been proposed: (i) *Giardia* may directly alter the epithelial barrier after a close interaction between the trophozoite and polarized intestinal cells, (ii) intestinal functions may be altered by factors secreted by *Giardia* including an 'enterotoxin', proteinases and lectins, and (iii) based on mouse studies, a mechanism involving the intervention of activated T lymphocytes. We used fully differentiated cultured human intestinal Caco-2/TC7 cells forming a monolayer and expressing several polarized functions of enterocytes of small intestine to investigate the mechanisms by which *G. intestinalis* induces structural and functional alterations in the host intestinal epithelium. We first report that adhesion of *G. intestinalis* at the brush border of enterocyte-like cells involves the lipid raft membrane microdomains of the trophozoite. We report an adhesion-dependent disorganization of the apical F-actin cytoskeleton that, in turn, results in a dramatic loss of distribution of functional brush border-associated proteins, including sucrase-isomaltase (SI), dipeptidylpeptidase IV (DPP IV) and fructose transporter, GLUT5, and a decrease in sucrose enzyme activity in *G. intestinalis*-infected enterocyte-like cells. We observed that the *G. intestinalis* trophozoite promotes an adhesion-dependent decrease in transepithelial electrical resistance (TER) accompanied by a rearrangement of functional tight junction (TJ)-associated occludin, and delocalization of claudin-1. Finally, we found that whereas the occludin rearrangement induced by *G. intestinalis* was related to apical F-actin disorganization, the delocalization of claudin-1 was not.**

Received 6 April, 2011; revised 8 June, 2011; accepted 7 July, 2011.
*For correspondence. E-mail vanessa.lievin-le-moal@u-psud.fr; Tel. (+33) 1 46 83 52 90; Fax (+33) 46 83 58 44.

Introduction

Giardia intestinalis (synonyms: *G. lamblia* and *G. duodenalis*), the aetiological agent of giardiasis, is a flagellated protozoan that specifically colonizes the small intestine of various vertebrates, including human beings. Giardiasis is one of the most common human intestinal diseases in both developing and developed countries (Müller and von Allmen, 2005; Lujan, 2006; Buret, 2007). *G. intestinalis* contributes to an estimated 280 million symptomatic human infections per year. However, most human *Giardia* infections result in no overt symptom, and are resolved spontaneously. In addition, *G. intestinalis* infection may facilitate the development of chronic enteric disorders, including inflammatory bowel disease, irritable bowel syndrome and various allergies (Buret, 2008).

Symptomatic giardiasis is characterized by severe and protracted watery diarrhoea, abdominal cramps, nausea, vomiting, malabsorption and weight loss. How the non-invasive *Giardia* spp. cause intestinal disease is not completely understood. The life cycle of *Gardia* spp. includes two main phases: the proliferative trophozoite phase and

the non-proliferative, infectious cyst phase (Ankarklev *et al*., 2010). The infection begins with the ingestion of cysts that lead to the release of excyzoites into the proximal region of the intestine, each of which immediately divides into four trophozoites (Bernander *et al*., 2001). During the initial proliferative stage, *Giardia* trophozoites form an adhesive ventral disk that adheres to the microvillous brush border of the small intestine, consisting of enterocytes (Palm *et al*., 2005). It is possible that the ventral disk and the brush border interact via receptor-ligand interaction(s) (Müller and von Allmen, 2005). *Giardia* induces a loss of epithelial barrier function and enterocyte injuries (Müller and von Allmen, 2005; Lujan, 2006; Buret, 2007; Ankarklev *et al*., 2010). Insights into whether *G. intestinalis* promotes structural and functional injuries in small intestinal epithelium have been obtained using rodent infection models (Belosevic *et al*., 1989; Buret *et al*., 1990; 1991; 1992; Daniels and Belosevic, 1992; 1995; Gorowara *et al*., 1992; Cevallos *et al*., 1995; Humen *et al*., 2005), cultured non-human and human intestinal cells (Chavez *et al*., 1986; Favennec *et al*., 1991; Teoh *et al*., 2000; Sousa *et al*., 2001; Scott *et al*., 2002) and human biopsies (Oberhuber *et al*., 1997; Singh *et al*., 2000; Teoh *et al*., 2000). In addition, although *Giardia* does not induce the production of pro-inflammatory cytokines (Jung *et al*., 1995), infected human intestinal cells display a particular profile of chemokines, substances that are involved in the recruitment of dendritic cells and can interfere with host's innate immunity, thus allowing the parasite to control the host's response (Roxstrom-Lindquist *et al*., 2005; Kamda and Singer, 2009). The mechanisms used by *G. intestinalis* to induce structural and functional alterations in the host intestinal epithelia remain unknown. It has been postulated that most of the *Giardia*-induced intestinal functional disorders result from brush border damage induced by *Giardia* (Müller and von Allmen, 2005; Buret, 2007). Three mechanisms have been proposed. According to the first mechanism, unidentified *Giardia* virulence factors directly alter the epithelial barrier after close interaction has occurred between the trophozoites and polarized intestinal cells. The second mechanism involves the intervention of activated T lymphocytes. The third mechanism involves factors secreted by *Giardia*, including an 'enterotoxin', proteinases and lectins. In the present study, we focused our investigation on the mechanism by which *G. intestinalis* promotes structural and functional cellular injuries after interaction has occurred between trophozoites and human intestinal cells. As our cellular model, we used human intestinal Caco-2/TC7 cells (Chantret *et al*., 1994), which spontaneously differentiate in culture to produce to a confluent cell monolayer that mimics the intestinal epithelial barrier (Pinto *et al*., 1983). Importantly, fully differentiated and polarized Caco-2/TC7 cells, although they are of colonic origin, express apical and basolateral proteins displaying the specific functions of enterocytes of the small intestine (Zweibaum *et al*., 1991). Many of the cellular and molecular mechanisms of enterovirulent microorganisms identified in non-polarized epithelial cells have been validated for the intestinal situation using this cell line (Lencer, 2001; Boyle and Finlay, 2003). Moreover, structural and functional alterations induced by enterovirulent bacteria and enteric viruses have recently been investigated using fully differentiated Caco-2 cells or clones. In order to evaluate the pathological mechanisms that lead to *G. intestinalis*-induced alterations in the host's epithelial structure and intestinal function, we assessed cell integrity, cell polarization, the cellular brush border cytoskeleton, the distribution of brush border enzymes, the integrity of the epithelial barrier and the distribution of functional tight junction (TJ) proteins. We provide evidence that both the structural and functional injuries promoted by *G. intestinalis* strains at the brush border of Caco-2/TC7 enterocyte-like cells and at the TJ of Caco-2/TC7 monolayers are adhesion-dependent. Moreover, we showed that adhesion-dependent induced disassembly in the apical F-actin cytoskeleton controls the loss of distribution of brush border-associated functional proteins including sucrase-isomaltase (SI), dipeptidylpeptidase IV (DPP IV) and the fructose transporter, GLUT5, and causes a decrease in sucrase enzyme activity. We demonstrate that *G. intestinalis* delocalizes the TJ-associated functional proteins, occluding and claudin-1. Finally, we observed that the disassembly of apical F-actin cytoskeleton plays a pivotal role in the rearrangement of the TJ-associated protein occludin, but not in the rearrangement of claudin-1.

Results

Trophozoite lipid rafts control the adhesion of G. intestinalis *to human enterocyte-like Caco-2/TC7 cells*

We examined the attachment capacity of *G. intestinalis* strains GS/H7, WB/C6 and WB/1267 to apically infected, fully differentiated Caco-2/TC7 cells. The number of trophozoites attached was determined 3 h post infection (p.i.), after infection with multiplicity of infection (moi) of 0.5, 1, 2 and 8 trophozoites per cell. Concentration-dependent adhesion was observed for all the strains examined (Fig. 1A). Strains GS/H7 and WB/C6 were highly adhesive, whereas strain WB/1267 displayed lower adhesion capability. Both the motility and ability to grow of adhering trophozoites were normal (not shown). A time-course infection with strain GS/H7 showed that the trophozoites adhered rapidly, and that adhesion levels did not evolve any further during the time-course of the infection (Fig. 1B).

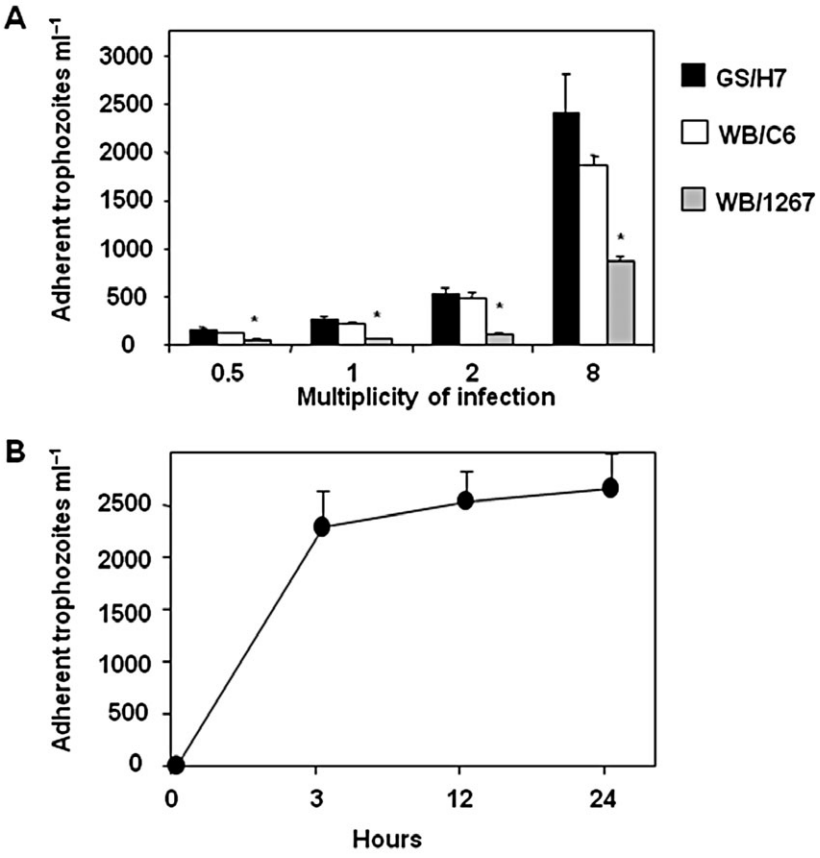

Fig. 1. Adhesion of *G. intestinalis* trophozoites to human enterocyte-like Caco-2/TC7 cell monolayers. After incubating for 3 h, the adhering trophozoites were counted as described in *Experimental procedures*.
A. Concentration-dependent adhesion of GS/H7, WB/C6 and WB/1267 trophozoites onto Caco-2/TC7 cells. Different amounts of trophozoites were added per well: 5×10^5, 1×10^6, 2×10^6 or 8×10^6 trophozoites ml^{-1}, with a multiplicity of infection (moi) of 0.5, 1, 2 and 8 respectively.
B. The time-course of GS/H7 trophozoite adhesion (moi, 8).
In (A), the asterisk (*) indicates a significant difference ($P < 0.05$) versus GS/H7 and GS/W6 at the same moi.

Lipid raft microdomains at the cell plasma membrane play a pivotal role in infectious processes (van der Goot and Harder, 2001). It has recently been reported that lipid rafts are involved in adhesion of *Entamoeba histolytica* trophozoites (Laughlin *et al*., 2004; Mittal *et al*., 2008). We investigated whether methyl-β-cyclodextrin (MBCD) (10 mM), a lipid raft disorganizing agent, affects the adhesion of *G. intestinalis* trophozoites to Caco-2/TC7 cells (Fig. 2). When cells were apically infected with cultures of *G. intestinalis* strains GS/H7, WB/C6 or WB/1267 in the presence of MBCD, we found that adhesion of trophozoites was abolished compared with untreated, infected cells (Fig. 2A). Since lipid rafts were present both in the cells and in the trophozoite membranes, we pre-treated either the Caco-2/TC7 cells or the *G. intestinalis* strain before the adhesion experiment. As shown in Fig. 2B, when the Caco-2/TC7 cells had been pre-treated with MBCD there was no inhibition of trophozoite adhesion compared with that of untreated cells. In contrast, when GS/H7, WB/C6 or WB/1267 trophozoites were pre-treated with MBCD before being used to infect Caco-2/TC7 cells, there was a complete inhibition of the adhesion (Fig. 2C). These findings constitute the first demonstration that *G. intestinalis* membrane rafts play a role in the adhesion of this organism to human, enterocyte-like cells.

The adhesion of G. intestinalis *disrupts the apical F-actin network in human enterocyte-like Caco-2/TC7 cells*

We investigated differences in the distribution of F-actin at the apical brush border of fully differentiated control Caco-2/TC7 cells and of Caco-2/TC7 cells infected with cultures of *G. intestinalis* GS/H7, WB/C6 and WB/1267 (moi 8, 24 h infection). Confocal laser microscopy scanning (CLMS) *x–y* images of F-actin labelled with fluorescein-labelled phalloidin in non-permeabilized cells (Fig. 3A) show that control cells displayed the typical mosaic pattern of microvillus-associated F-actin due to the different morphologies of microvilli in fully differentiated Caco-2 cells (Peterson and Mooseker, 1992; Peterson *et al*., 1993). In contrast, Caco-2/TC7 cells apically infected with *G. intestinalis* GS/H7 and WB/C6 showed a dramatic alteration of the distribution of F-actin (Fig. 3A). F-actin immunolabelling revealed central translucent zones, with the accumulation of F-actin at cell-to-cell contact points. In addition, vacuole-like structures were observed in infected cells. In WB/1267-infected cells, mildly impaired apical distribution of F-actin was observed (Fig. 3A). Quantification of the F-actin labelling confirms that F-actin distribution was less affected in

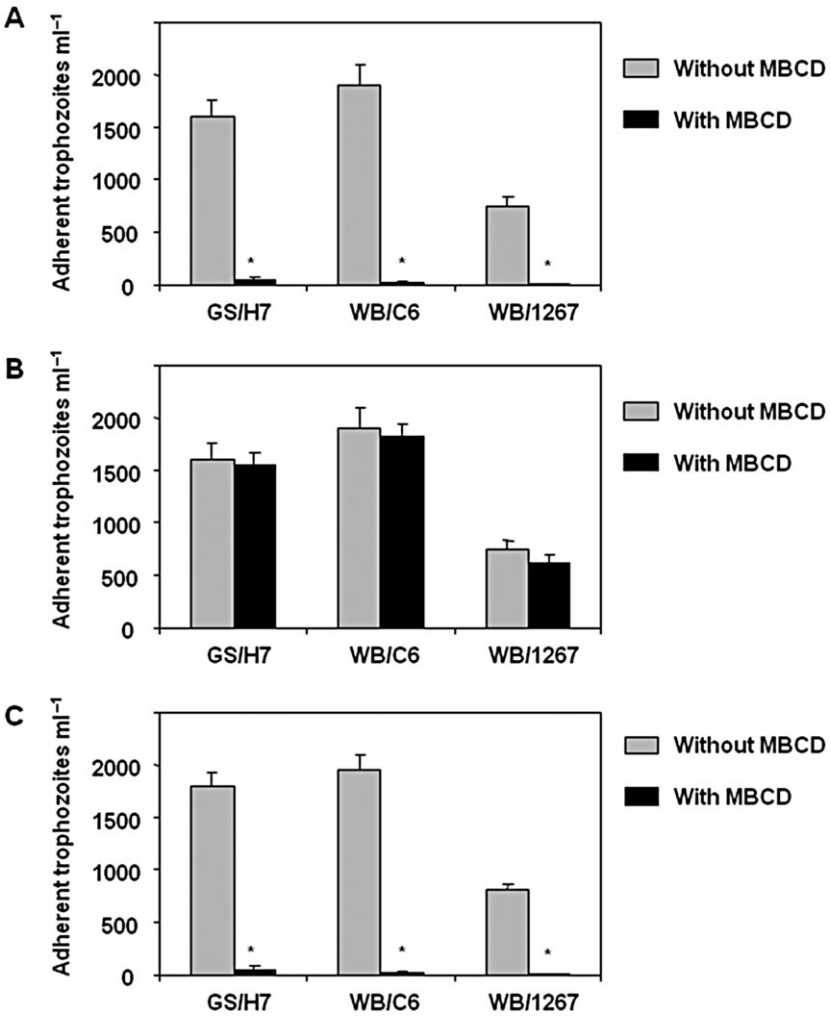

Fig. 2. Treatment of *G. intestinalis* GS/H7 trophozoites with the lipid raft-destabilizing agent, methyl-β-cyclodextrin (MBCD) inhibits their adhesion to Caco-2/TC7 cells.
A. Adhesion of GS/H7 trophozoites with or without MBCD in the incubation medium.
B. Adhesion of GS/H7 trophozoites to Caco-2/TC7 cells with or without MBCD pre-treatment of cells.
C. Adhesion of untreated and MBCD-treated (10 mM) GS/H7 trophozoites to Caco-2/TC7 cells.
All data are the means (SEM) of three independent experiments. In (B) and (C), The asterisks indicate a significant difference ($P < 0.01$) versus control cells without MBCD treatment.

WB/1267-infected cells, than in GS/H7- and WB/C6-infected cells (Fig. 3B).

These findings prompted us to examine in greater detail the localization of F-actin within fully differentiated control Caco-2/TC7 cells and in *G. intestinalis*-infected Caco-2/TC7 cells. To do this, cells were infected with *G. intestinalis* strain GS/H7 (moi 8, 24 h infection). The F-actin network was examined by direct labelling of Triton-permeabilized cells with fluorescein-labelled phalloidin and CLMS analysis. As shown in Fig. 3C, the control cell monolayers displayed the typical regular organization of fully differentiated Caco-2/TC7 cells, with F-actin localized apically at the brush border and laterally at cell-to-cell contact points in polarized cells (Peterson and Mooseker, 1992; Peterson *et al*., 1993). The cell-to-cell contacts expressing F-actin were still present in cells apically infected with *G. intestinalis* GS/H7 (Fig. 3C), indicating that the polarized organization of the cells had not been altered. Consistent with this, no signs of any disruption of cell integrity were observed when assessed by determining LDH activity in the supernatant, cell detachment and necrosis (data not shown). However, the GS/H7-infected cell monolayers appeared to have been dramatically altered, with irregular cell sizes compared with the control cells. In particular, in some infected cells the apical domain was rounded, and F-actin labelling at the brush border was irregular compared with that in control cells. Comparison of the sizes of the apical F-actin bands by CLMS and image analysis shows that, in control cells, the F-actin labelling was distributed as a homogeneous band measuring 4.8 ± 0.2 μm. In contrast, in GS/H7-infected cells the apical the F-actin labelling was irregular, forming a band of $\sim 2.3 \pm 0.7$ μm (P-value < 0.01).

F-actin immunolabelling was examined in fully differentiated cells infected with *G. intestinalis* strain GS/H7-infected (moi 8), during a time-course of infection. Surprisingly, we observed no change in the distribution of brush border-associated F-actin in non-permeabilized, infected cells 3 h or 12 h p.i. (Fig. 3D) compared with that in infected cells at 24 h p.i., despite the fact that similar trophozoite adhesion to Caco-2/TC7 cells was seen 3 h, 12 h and 24 h p.i. (Fig. 1B).

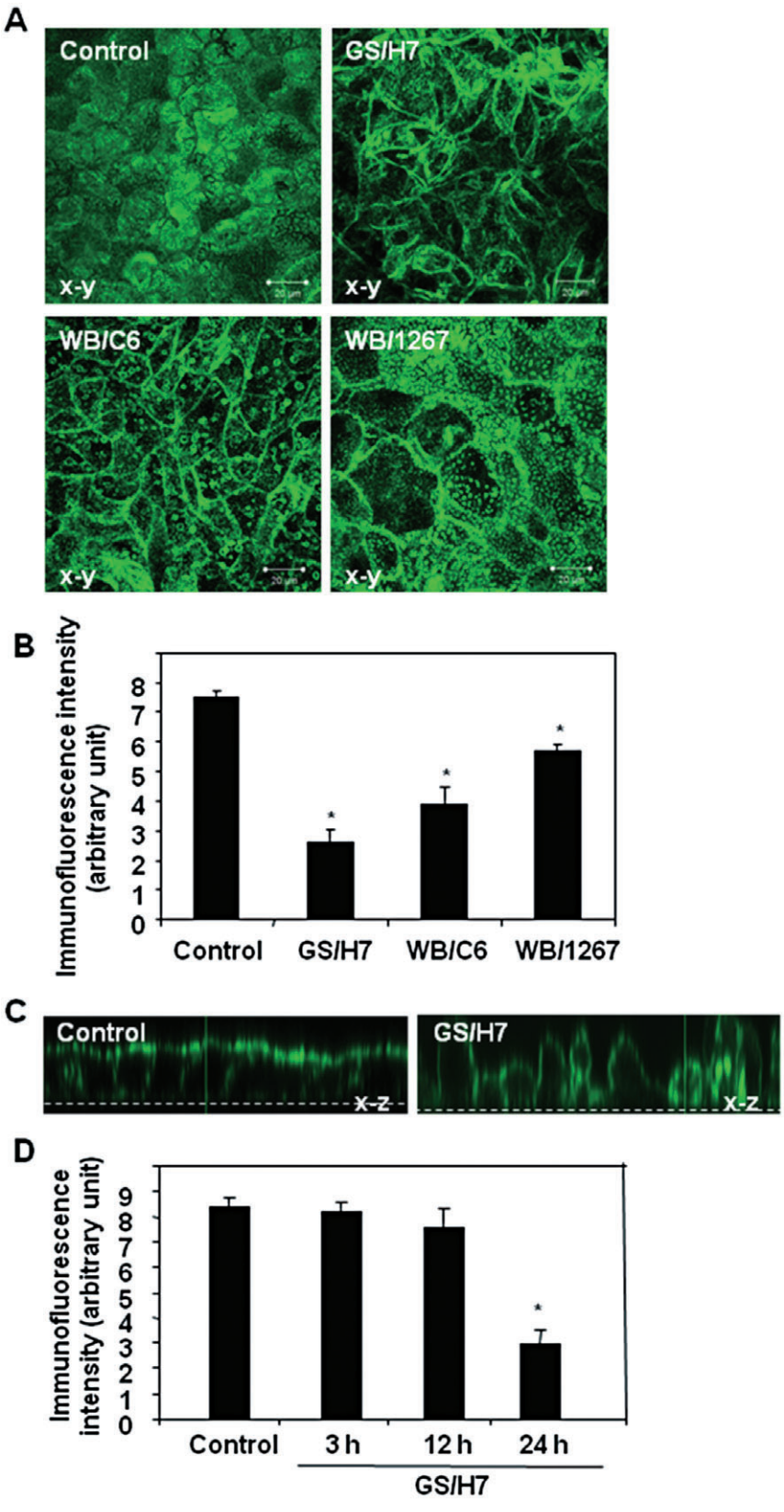

Fig. 3. Distribution of F-actin in human enterocyte-like Caco-2/TC7 cell monolayers infected with *G. intestinalis* strains. After infection, the cells were fixed, permeabilized with Triton X-100 (or not), and processed for direct immunofluorescence labelling of F-actin with fluorescein-phalloidin as described in *Experimental procedures*, and observed by CLMS microscopy.
A. F-actin immunofluorescence in non-permeabilized control cells, and cells apically infected *G. intestinalis* trophozoites strains GS/H7, WB/C6 and WB/1267 (moi = 8) (horizontal *x–y* optical sections).
B. Quantification of F-actin immunofluorescence by CLMS analysis in non-permeabilized control cells and in *G. intestinalis*-infected cells.
C. Lateral views show the cell distribution of F-actin obtained by CLMS analysis (vertical *x–z* optical section) in Triton X-100-permeabilized control cells and in cells infected with *G. intestinalis* strain GS/H7 (moi = 8; 24 h of infection).
D. Quantification of F-actin immunofluorescence by CLMS analysis in non-permeabilized control cells and in *G. intestinalis* GS/H7-infected cells during a time-course of infection. Samples were analysed by serial optical horizontal sectioning, starting at the basal level of the cells until the apical level (horizontal *x–y* optical sections).
In (C), the hatched line indicates the basal domain of the polarized cell monolayer. In (A) and (C), the micrographs are representative of three independent experiments. Data in (B) and (D) are the mean values (SEM) of three independent experiments. The asterisk (*) represents a significant difference ($P < 0.01$) versus control cells.

The adhesion of G. intestinalis *dramatically modified the distribution of the brush border enzymes, of SI and of the fructose transporter GLUT5*

Functional proteins with specific intestinal functions are known to be localized at the brush border of cultured human enterocytes (Peterson and Mooseker, 1992; Peterson *et al*., 1993). Since modification of the brush border cytoskeleton could lead to functional deficiencies, we analysed the distribution of brush border enzymes and transporters in GS/H7-infected cells. The enzymes and transporters investigated included SI, an α-glycosidase that hydrolyses maltose, sucrose and maltotriose, DPP IV, a widely distributed membrane glycoprotein essential for the transport of proline-containing peptides, and the transporter GLUT5, which is required for the active transport of fructose (Fig. 4). The immunofluorescent labelling of SI in non-permeabilized GS/H7-infected cells at 24 h p.i. shows that a high proportion of the infected cells had lost the mosaic pattern of SI immunofluorescence, which had been replaced by small, SI-positive puncta (Fig. 4A and B). In the same way, GS/H7-infected cells showed a dramatic reduction in the brush border-associated transporter GLUT5 as compared with uninfected cells (Fig. 4A and B). In contrast, the distribution of DPP IV was modified after infection to a lesser extent than that of SI or GLUT5 (Fig. 4A and B). Correlating with this modification of the SI distribution, we observed a dramatic decrease in the brush border membrane-associated sucrase activity in *G. intestinalis* GS/H7-infected Caco-2/TC7 cells compared with that in control cells (Table 1). We further examined SI and GLUT5 immunolabelling at the brush border of non-permeabilized cells during the time-course of infection with strain GS/H7 (moi 8). As observed above for F-actin (Fig. 3D), we saw no change in the distribution of SI or GLUT5 at the brush border of the infected GS/H7-infected cells 3 h and 12 h p.i. (Fig. 4C) compared with infected cells at 24 h p.i.

Since several authors have variously linked giardiasis to iron, haemoglobin and transferrin deficiencies (Sackey *et al*., 2003; Monajemzadeh and Monajemzadeh, 2008), we investigated whether *G. intestinalis* strain GS/H7 induces any modification in the transferrin receptor distribution. There was no difference between infected and control cells with regard to the distribution of the transferrin receptor (not shown).

Table 1. Adhesion- and lipid raft-dependent reduction of sucrase activity in the brush border of *G. intestinalis* GS/H7-infected enterocyte-like Caco-2/TC7 cells.

	Sucrase enzyme activity (mU per mg protein)
Control	155 ± 4
GS/H7	32 ± 4*
Control + MBCD (10 mM)	150 ± 3
GS/H7 + MBCD (10 mM)	152 ± 7**
Control + JAS (1 μM)	148 ± 5
GS/H7 + JAS (1 μM)	147 ± 12**

moi = 8, after 24 h of infection. *$P < 0.01$ versus control. **$P < 0.01$ versus GS/H7.

Inhibition of adhesion and stabilization of the cytoskeleton antagonize the G. intestinalis *GS/H7-induced impairment of SI distribution and activity*

We investigated whether the *G. intestinalis*-induced structural and functional changes observed above in Caco-2/TC7 cell monolayers are related to trophozoite adhesion or not. We checked whether the above-observed effects on F-actin, SI and GLUT5 distribution were related to substances secreted by *G. intestinalis*. When Caco-2/TC7 cells were incubated for 24 h in the presence of a cell-free, spent culture supernatant of strain GS/H7, the distributions of F-actin, SI, DPP IV and GLUT5 were the same as those following incubation in the presence of a GS/H7 culture (Fig. 5A). In order to check that the adhesion of GS/H7 trophozoites determined the structural and functional changes observed above with GS/H7 culture, we used MBCD to inhibit the adhesion of *G. intestinalis* trophozoites. When Caco-2/TC7 cells were apically infected for 24 h with MBCD-treated *G. intestinalis* GS/H7 trophozoites (moi = 8), CLMS analysis of infected cells showed that the distribution of apical F-actin cytoskeleton, SI and GLUT5 was the same as that in cells infected with untreated GS/H7 (Fig. 5B and C). We also found no difference between the sucrase activity in the brush border membrane of Caco-2/TC7 cells infected with MBCD-treated GS/H7 and that of cells infected with untreated GS/H7 (Table 1).

It has previously been reported that the functionality of brush border-associated proteins is dependent on the establishment and maintenance of the polarized organization of the cells, which is controlled by the cytoskeleton (Peterson and Mooseker, 1993; Peterson *et al*., 1993). In order to demonstrate whether the *G. intestinalis*-induced functional injuries reported above are directly related to cytoskeleton disorganization, we conducted experiments in which the cytoskeleton was stabilized before infection. To do this, we used jasplakinolide (JAS) (1 μM), an F-actin-stabilizing agent to protect the cell cytoskeleton in Caco-2/TC7 cells infected with an enterovirulent *Escherichia coli* (Peiffer *et al*., 2001). In a preliminary experiment, we checked that the JAS treatment had no effect on the adhesion of *G. intestinalis* GS/H7 to Caco-2/TC7 cells (not shown) and as expected, found that it did not modify the apical distribution of F-actin and SI in uninfected cells (Fig. 6A). We observed that the apical distribution of F-actin, SI and GLUT5 was the same in JAS-treated *G. intestinalis* GS/H7-infected cells as in

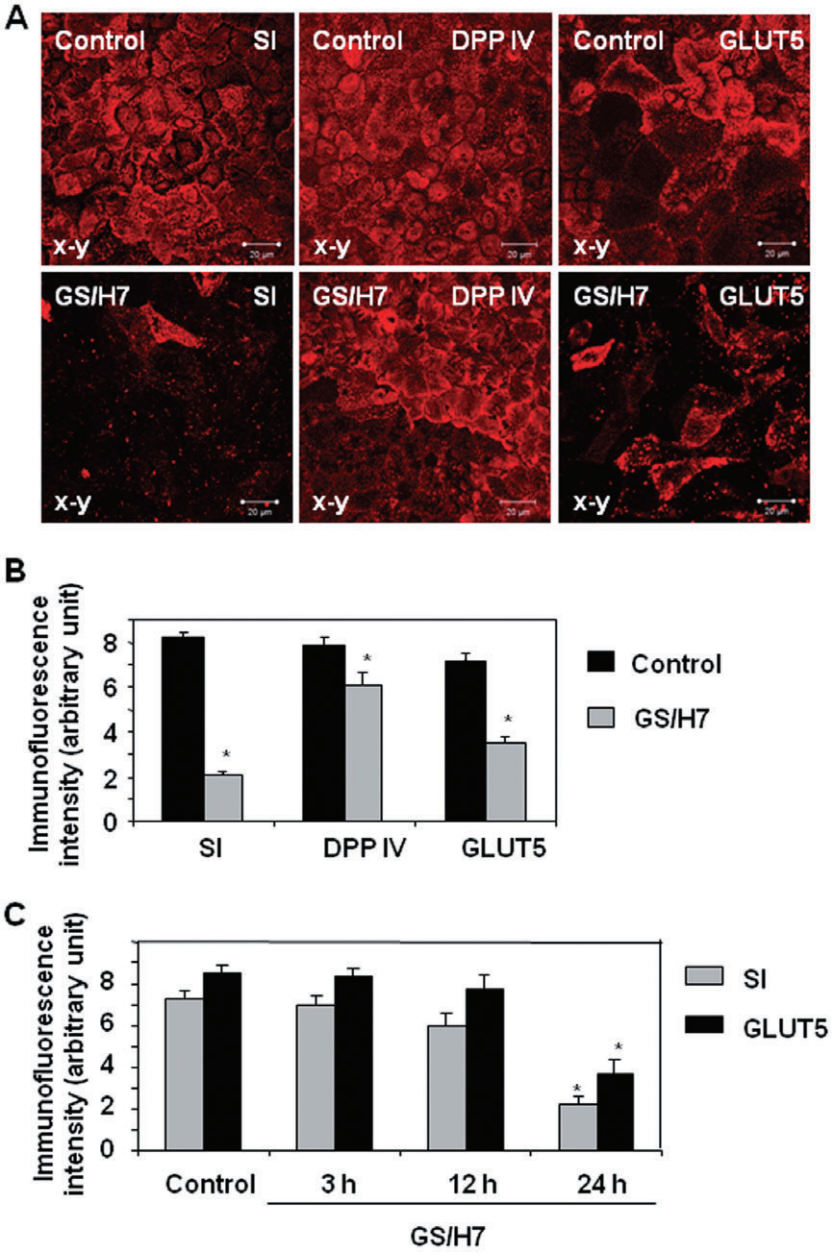

Fig. 4. Changes in the distribution of brush border-associated functional proteins in *G. intestinalis* GS/H7-infected human enterocyte-like Caco-2/TC7 cell monolayers. Cells were apically infected for 24 h with *G. intestinalis* trophozoites strain GS/H7 (moi = 8). Cells were processed for direct F-actin labelling or indirect immunofluorescence labelling of SI, DPP IV and GLUT5 in non-permeabilized cells, as described in *Experimental procedures*.

A. Distribution of SI, DPP IV and GLUT5 in control and GS/H7-infected cells. CLMS analysis was carried out to obtain *en face* micrographs (horizontal *x–y* optical sections).

B. Quantification of SI, DPP IV and GLUT5 immunofluorescence by CLMS analysis in control cells and *G. intestinalis*-infected cells.

C. Quantification of SI and GLUT5 immunofluorescence by CLMS analysis in non-permeabilized control cells and *G. intestinalis* GS/H7-infected cells during a time-course of infection.

In (A), the micrographs are representative of three independent experiments. Data in (B) and (C) are the means (SEM) of three independent experiments. The asterisk (*) represents significant differences ($P < 0.01$) versus control.

untreated *G. intestinalis* GS/H7-infected cells (Fig. 6A and B). Consistently with the CLMS examination, we observed that sucrase activity in the brush border membrane of JAS-treated, GS/H7-infected Caco-2/TC7 cells was the same as that of control uninfected cells and non-JAS-treated GS/H7-infected cells (Table 1). Taken together, these results showed that the GS/H7-induced structural and functional brush border injuries are both adhesion-

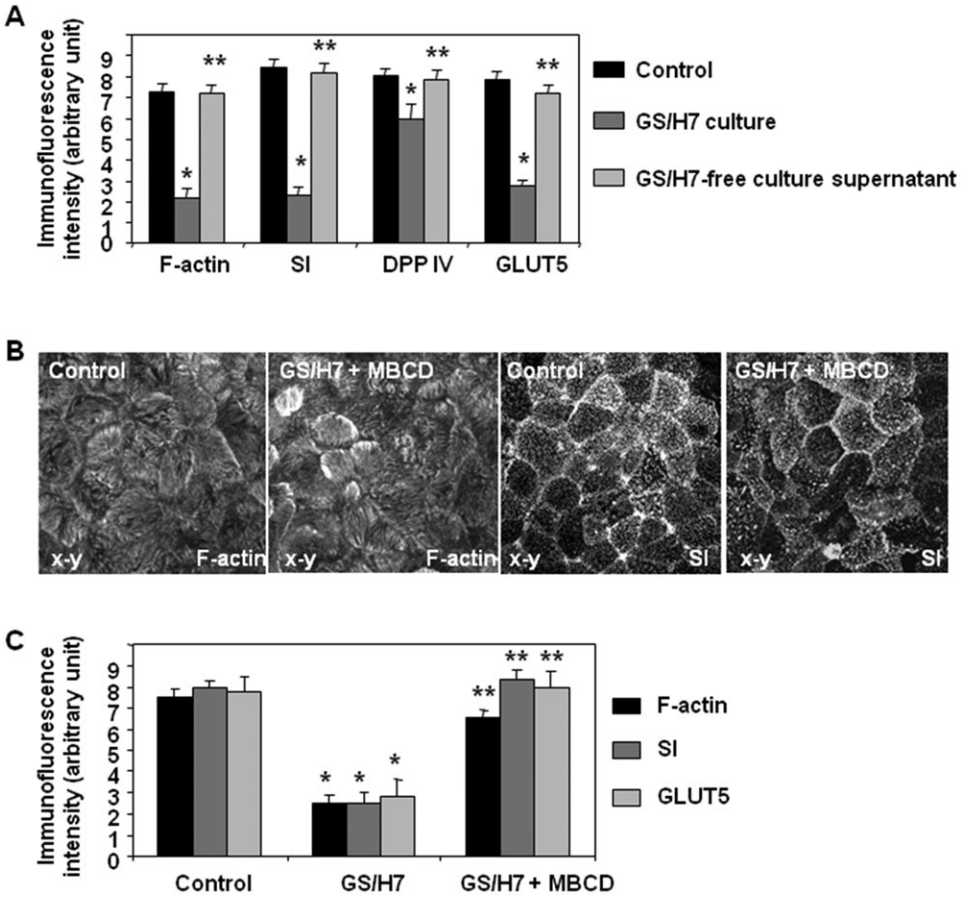

Fig. 5. *G. intestinalis*-induced structural and functional injuries at the apical of Caco-2/TC7 cells were adhesion-dependent. GS/H7 trophozoites were seeded per well: $8{\cdot}10^6$ trophozoites ml^{-1} (moi = 8). Cells were infected for 24 h, and processed for direct labelling or indirect immunofluorescence labelling for CLMS examination of F-actin, SI, DPP IV and GLUT5 as described in *Experimental procedures*.
A. Quantification of F-actin, SI, DPP IV and GLUT5 immunofluorescence in control cells and cells infected with a GS/H7 culture or a trophozoite-free supernatant of a GS/H7 culture (TYI : DMEM in a 50:50 ratio).
B. CLMS observation of F-actin and SI in control Caco-2/TC7 cells and in cells infected with untreated or MBCD (10 mM)-treated *G. intestinalis* GS/H7.
C. Quantification of F-actin, SI and GLUT5 immunofluorescence in control Caco-2/TC7 cells and in cells infected with untreated or MBCD (10 mM)-treated *G. intestinalis* GS/H7.
CLMS analysis was carried out to obtain *en face* micrographs (horizontal *x–y* optical sections). In (B), the micrographs are representative of three independent experiments. Data in (A) and (C) are the means (SEM) of three independent experiments. In (A), the asterisk (*) indicates a significant difference ($P < 0.01$) versus control, and the double asterisk (**) indicates a significant difference ($P < 0.01$) versus the GS/H7 culture. In (C), the asterisk (*) indicates a significant difference ($P < 0.01$) versus control, and the double asterisk (**) indicates a significant difference ($P < 0.01$) versus GS/H7.

dependent. Our findings also demonstrate that GS/H7-induced changes in the distribution and activity of brush border-associated SI hydrolase and GLUT5 transporter are dependent on the GS/H7-induced disassembly of the F-actin cytoskeleton.

G. intestinalis *induces alterations in the distribution of the TJ-associated functional proteins, occludin and claudin-1*

Previous reports have shown that decreased TER results from alterations of the TJ-associated proteins, ZO-1 and claudin-1, after *Giardia* infection of cell monolayers (Buret *et al*., 2002; Scott *et al*., 2002) and in human biopsy specimens from patients with chronic giardiasis (Troeger *et al*., 2007). We confirmed that a decrease in TER develops in Caco-2/TC7 cell monolayers infected with *G. intestinalis* strains GS/H7, WB/C6 or WB/1267 (moi = 8, 24 h of infection) (Table 2). Time-course monitoring of TER in *G. intestinalis* GS/H7-infected Caco-2/TC7 cell monolayers showed a time-dependent decrease of TER starting at 12 h p.i. (control: 774 ± 29; GS/H7 3 h p.i. 771 ± 32; GS/H7 12 h p.i. 585 ± 45; GS/H7 24 h p.i. $350 \pm 23\ \Omega\ cm^2$). We conducted an in-depth analysis of the distribution of two functional TJ-associated proteins: occludin (Furuse *et al*., 1993) and claudin-1 (Furuse *et al*.,

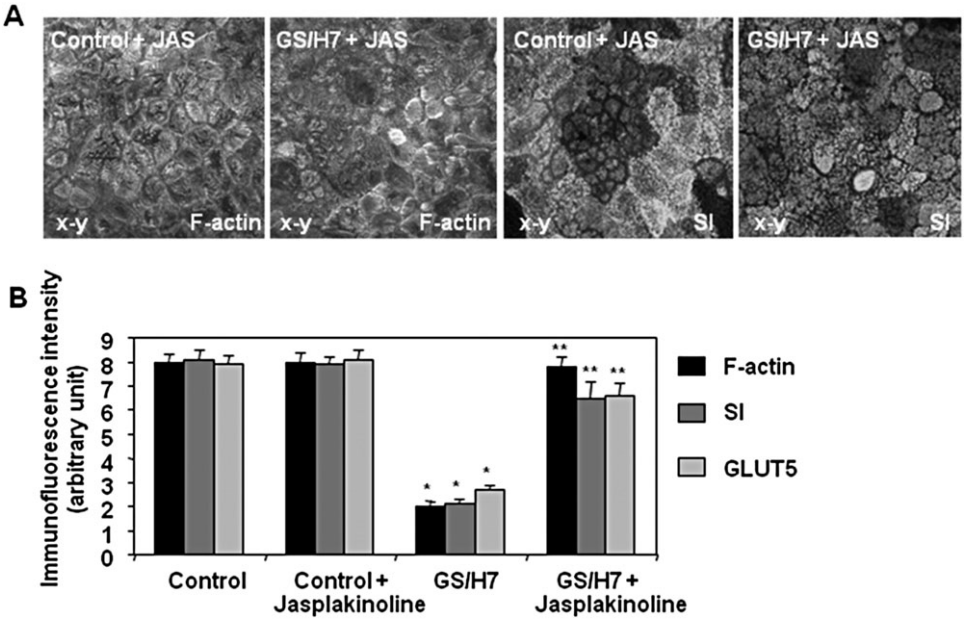

Fig. 6. Treatment of Caco-2/TC7 cell monolayers with the cytoskeleton-stabilizing agent jasplakinolide (JAS) abolishes the *G. intestinalis* GS/H7-induced disassembly of the F-actin cytoskeleton, and the loss of distribution of the brush border-associated functional proteins, SI and GLUT5. Cells pre-treated with JAS (1 μM) or untreated were apically infected for 24 h with *G. intestinalis* strain GS/H7 trophozoites (moi = 8). Cells were processed for immunofluorescence labelling of F-actin, DPP IV and GLUT5, as described in *Experimental procedures*. CLMS analysis was carried out to obtain *en face* micrographs (horizontal *x–y* optical sections), and the quantification of F-actin, SI and GLUT5 immunofluorescence.

A. CLMS observation of F-actin and SI in Caco-2/TC7 cells treated with JAS and in JAS-treated cells infected with *G. intestinalis* GS/H7.

B. Quantification of F-actin, SI and GLUT5 immunofluorescence in Caco-2/TC7 cells treated with JAS and in JAS-treated cells infected with *G. intestinalis* GS/H7.

All data are means (SEM) of three independent experiments. In (B), the asterisk (*) represents a significant difference ($P < 0.01$) versus control, and the double asterisk (**) represents a significant difference ($P < 0.01$) versus GS/H7.

1998) in *G. intestinalis*-infected Caco-2/TC7 cell monolayers (moi = 8, 24 h of infection). Indirect immunolabelling of occludin and CLMS analysis showed that the protein was localized at cell-to-cell contact points in uninfected Caco-2/TC7 cells, and the typical honeycomb-like pattern can be observed (Fig. 7A). In contrast, apical infection of Caco-2/TC7 cell monolayers with *G. intestinalis* strains GS/H7, WB/C6 or WB/1267 induced modification of the cell-to-cell organization characterized by an obvious loss of the typical honeycomb structure (Fig. 7A). Occludin distribution was modified, now showing a brightly stained continuous band lining each cell-to-cell contact.

Table 2. Decrease of TER in the *G. intestinalis* GS/H7-infected enterocyte-like Caco-2/TC7 cell monolayer.

	TER (Ω cm^2)
Control	774 ± 29
GS/H7	355 ± 21*
Control + MBCD (10 mM)	765 ± 25
GS/H7 + MBCD (10 mM)	735 ± 28**
Control + JAS (1 μM)	768 ± 21
GS/H7 + JAS (1 μM)	692 ± 32**

moi = 8, after infection for 24 h. *$P < 0.01$ versus control. **$P < 0.01$ versus GS/H7.

Phosphorylated and non-phosphorylated forms of occludin have both been described (Farshori and Kachar, 1999). It has been established that non-phosphorylated occludin has a cytoplasmic localization, and that it is easily extracted using Triton X-100. In contrast, phosphorylated occludin, located at cell-to-cell contact points, is resistant to extraction with Triton X-100. Occludin distribution was analysed by Western blotting of Triton X-100-soluble and Triton X-100-resistant fractions of *G. intestinalis* GS/H7-infected Caco-2/TC7 cells. In Triton X-100-soluble fractions (Fig. 7B), a 65 kDa band corresponding to the non-phosphorylated form of occludin was observed. A densitometric analysis of the Triton X-100-soluble fraction of *G. intestinalis* GS/H7-infected cells revealed that non-phosphorylated occludin was significantly lower ($P < 0.05$) in these cells than in the control cells (Fig. 7C). In the Triton X-100-resistant fraction (Fig. 7B), two bands were observed corresponding to the non-phosphorylated (65 kDa) and phosphorylated (72 kDa) forms of occludin respectively. Quantification of non-phosphorylated occludin in the Triton X-100-resistant fraction of *G. intestinalis* GS/H7-infected cells did not reveal any statistical difference from control cells (Fig. 7C). In contrast, the Triton X-100-resistant fraction of

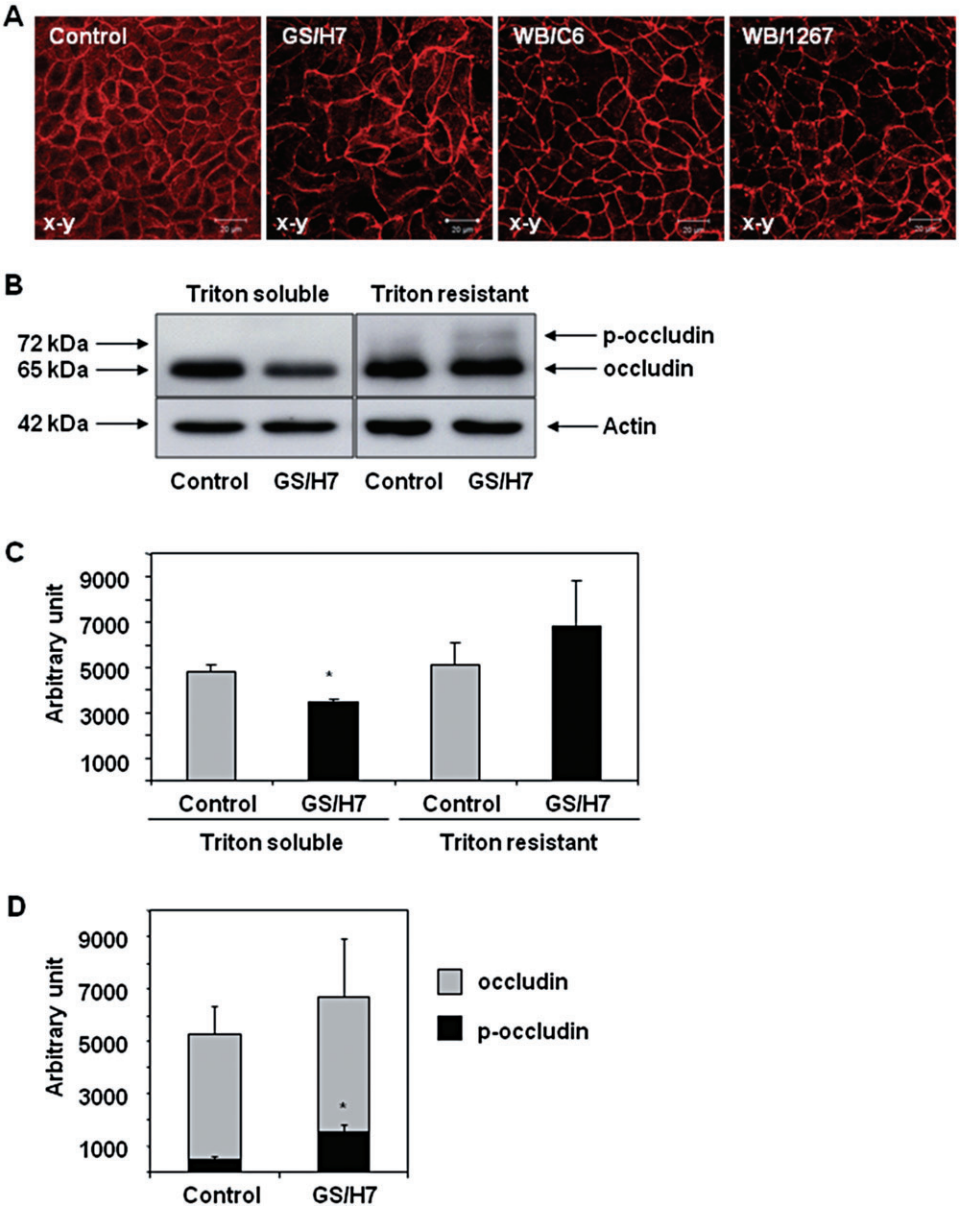

Fig. 7. Changes in the distribution of the tight junction-associated protein, occludin, in *G. intestinalis*-infected human enterocyte-like Caco-2/TC7 cells. Cells were apically infected with trophozoites of *G. intestinalis* strains GS/H7, WB/C6 and WB/1267 for 24 h ($8{\cdot}10^6$ trophozoites ml^{-1}, moi = 8).

A. Control and infected cells were processed for indirect immunofluorescence labelling of occludin as described in *Experimental procedures*. CLMS analysis was carried out to obtain *en face* micrographs (horizontal *x–y* optical sections).

B. Distribution of the non-phosphorylated and phosphorylated forms of occludin in Triton X-100-soluble and Triton X-100-resistant fractions isolated from uninfected or *G. intestinalis* GS/H7-infected cells. Fractions were analysed by SDS-PAGE and Western blot. The phosphorylated occludin (p-occludin) band (72 kDa), and the non-phosphorylated occludin band (65 kDa) are shown. Actin (42 kDa) was used as the normalization parameter.

C. Densitometry analysis of Triton X-100-soluble and Triton X-100-resistant fractions of uninfected control cells and of cells infected with *G. intestinalis* GS/H7.

D. Densitometry analyses of occludin (grey bars) and p-occludin (black bars) in Triton X-100-resistant fractions of uninfected control cells and of cells infected with *G. intestinalis* GS/H7-.

All data are the means (SEM) of three independent experiments. The asterisk (*) indicates a significant difference ($P < 0.05$) versus uninfected control cells. The micrographs are representative of three independent experiments. Immunoblots are representative of three independent experiments.

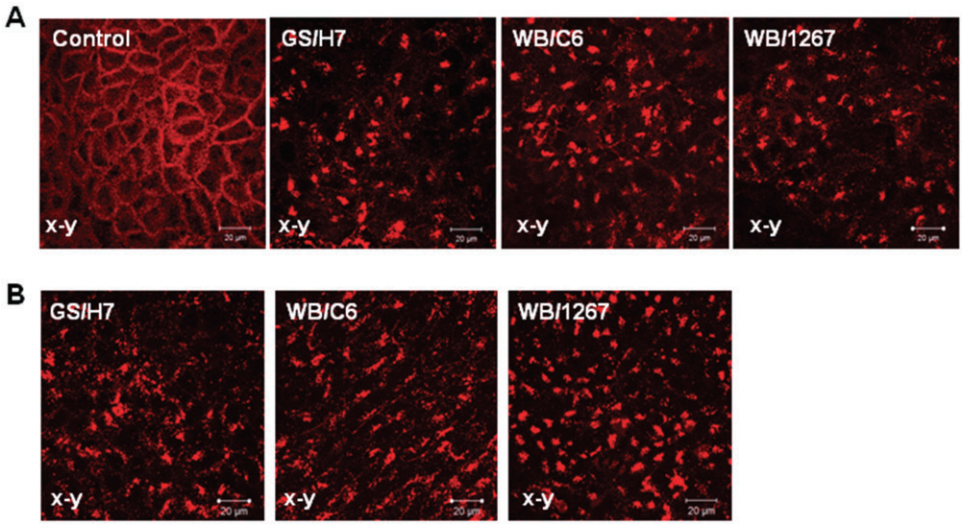

Fig. 8. Changes in the distribution of the tight junction-associated protein, claudin-1, in *G. intestinalis*-infected human enterocyte-like Caco-2/TC7 cell monolayers. Cells were apically infected with trophozoites of *G. intestinalis* strains GS/H7, WB/C6 and WB/1267 for 24 h ($8{\cdot}10^6$ trophozoites ml^{-1}, moi = 8). Cells were processed for indirect immunofluorescence labelling of claudin-1, as described in *Experimental procedures*.
A. Control cells and cells infected apically with trophozoites of *G. intestinalis* strains GS/H7, WB/C6 and WB/1267.
B. Infected cells were processed for the indirect immunofluorescence labelling of claudin-1 after treatment with Triton X-100.
CLMS analysis was carried out to obtain *en face* micrographs (horizontal *x–y* optical sections). The micrographs are representative of three independent experiments.

G. intestinalis GS/H7-infected cells contained more of the phosphorylated form of occludin than the control cells ($P < 0.05$) (Fig. 7B and D).

The differential expression of claudins 1, 2, 3, 4, 5, 6, 7 and 8 had previously been reported depending on the Caco-2 cell clones used. Depletion of Caco-2 cell cholesterol with MBCD resulted in the displacement of claudins 3, 4 and 7, but not of claudin 1, from the cholesterol-rich domains (Lambert *et al.*, 2007). Since MBCD treatment was used in our experiments, we decided to examine claudin-1 distribution in Caco-2/TC7 cells infected for 24 h with *G. intestinalis* strain GS/H7, WB/C6 or WB/1267 trophozoites. In the control cells, claudin-1 was seen at the cell-to-cell contact points (Fig. 8A). In contrast, there was a total loss of the claudin-1 immunolabelling at cell-to-cell contacts between infected cells, and claudin-1 was localized within small aggregates in the central region (Fig. 8A). The GS/H7-, WB/C6- and WB/1267-infected cells subjected to Triton X-100 treatment showed that the delocalized, centrally expressed, claudin-1 aggregates were resistant to extraction with the detergent (Fig. 8B).

Next to the TJs lies the *adherens junction* that orchestrates the intercellular junction, thereby playing a pivotal role in establishing and maintaining the epithelial architecture. Examining the distribution of the *adherens junction*-associated protein, E-cadherin, we observed that the *Giardia* infection did not modify the distribution of this protein (not shown), suggesting that the polarized organization of the Caco-2/TC7 cell monolayer was not modified after *Giardia* infection.

We then investigated whether inhibition of the adhesion of *G. intestinalis* GS/H7 trophozoites by MBCD and/or stabilization of the F-actin cytoskeleton by JAS modified the GS/H7-induced changes in TER, or the distribution of occludin and claudin-1. The results shown in Table 2 show that no *G. intestinalis* GS/H7-induced decrease in TER occurred when the GS/H7 trophozoites were treated before infection with MBCD or when the Caco-2/TC7 cells were pre-treated with JAS before infection. As shown in Fig. 9, both MBCD treatment (Fig. 9A) and JAS treatment (Fig. 9B) abolished the GS/H7-induced rearrangement of occludin. MBCD treatment of cells also abolished the GS/H7-induced delocalization of claudin-1. Surprisingly, JAS treatment of cells did not modify the GS/H7-induced delocalization of claudin-1. Overall, these results show that both the GS/H7-induced rearrangement of occludin and the delocalization of claudin-1 are adhesion-dependent. Interestingly, we found that the adhesion-dependent GS/H7-induced rearrangement of occludin resulted of GS/H7-induced disassembly of the F-actin cytoskeleton, whereas the GS/H7-induced delocalization of claudin-1 did not.

Discussion

The intestinal polarized cells that make up the epithelium provide physical and chemical barriers that protect the

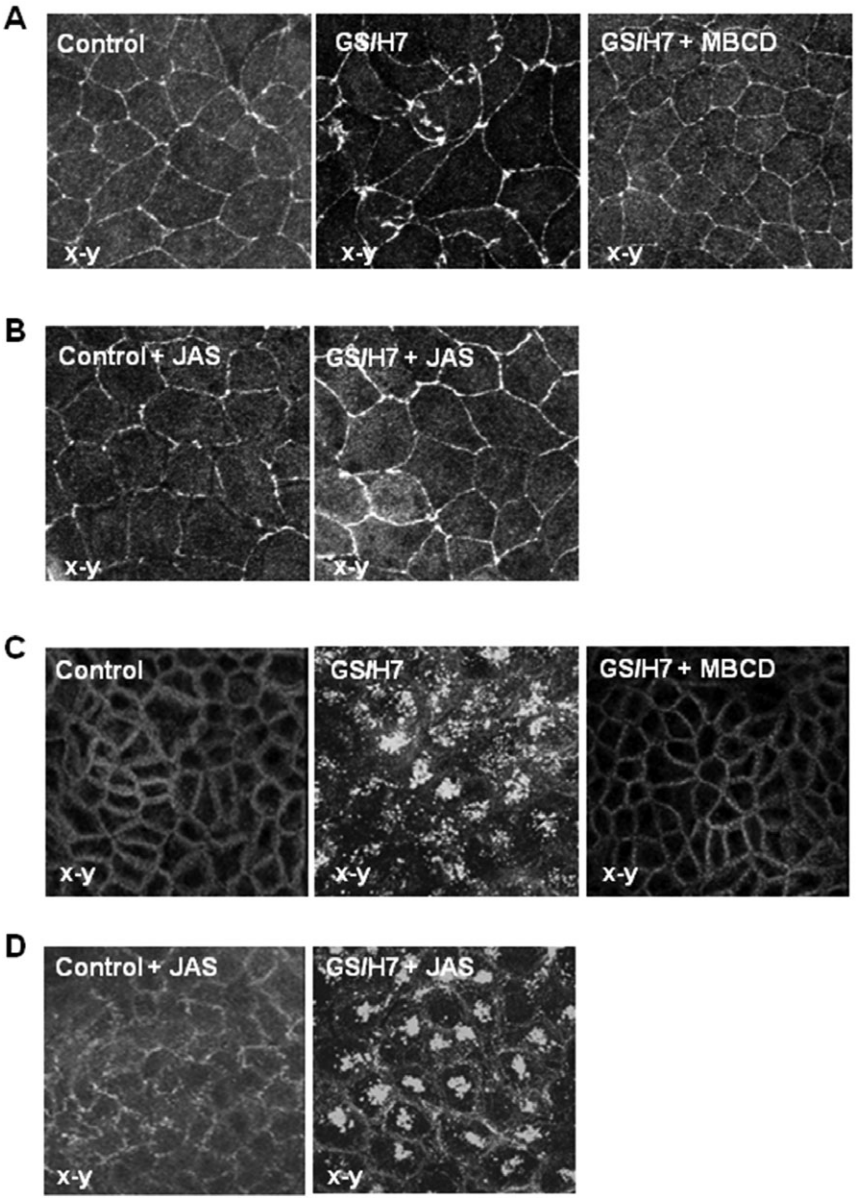

Fig. 9. Inhibition of *G. intestinalis* GS/H7 adhesion to human enterocyte-like Caco-2/TC7 cell monolayers by MBCD treatment of trophozoites abolishes both the trophozoite-induced rearrangements in the distributions of occludin and claudin-1, and stabilization of the F-actin cytoskeleton by jasplakinolide treatment of cells had no effect on claudin-1 rearrangement, but inhibited the rearrangement of occludin. Cells were apically infected with trophozoites of *G. intestinalis* strains GS/H7, WB/C6 and WB/1267 for 24 h ($8{\cdot}10^6$ trophozoites ml^{-1}, moi = 8). Cells were processed for the indirect immunofluorescence labelling of occludin and claudin-1, as described in *Experimental procedures*.
A. Occludin distribution in non-infected, control cells and in cells infected with trophozoites, which had or had not been treated with MBCD (10 mM).
B. Distribution of occludin in control cells and in GS/H7-infected cells treated with JAS (1 μM).
C. Claudin-1 distribution in uninfected control cells and cells infected with trophozoites, which had or had not been treated with MBCD (10 mM).
D. Claudin-1 distribution in control cells and in GS/H7-infected cells treated with JAS (1 μM).
CLMS analysis was carried out to obtain *en face* micrographs (horizontal *x–y* optical sections). The micrographs are representative of three independent experiments.

host against the unwelcome intrusion of microorganisms (Lievin-Le Moal and Servin, 2006). The adhesion of *G. intestinalis* trophozoites to epithelial intestinal cells is the first step in the pathogenesis of intestinal disease. There is evidence showing that this adhesion step is a multi-factorial process that involves flagella motility, mechanical forces of the ventral disk and of the ventrolateral border structures, and surface molecules (Ankarklev *et al*., 2010). Previous studies have demonstrated the role of *G. intestinalis* surface lectins in the attachment of trophozoites to epithelial host cells (Pegado and de Souza, 1994; Katelaris *et al*., 1995; Sousa *et al*., 2001). We describe here for the first time that disruption of *G. intestinalis* trophozoites lipid rafts by MBCD treatment leads to the inhibition of adhesion of trophozoites at the brush border, and from the abolition of the *G. intestinalis*-induced structural and functional injuries in cultured enterocyte-like cells. Subdomains in cell membranes created by lipid–lipid and protein–lipid interactions are referred to as membrane lipid rafts rich in phospholipids, glycosphingolipids and cholesterol. Lipid rafts contain glycosylphosphatidylinositol-anchored proteins, and several studies have shown that myristoylation and palmitoylation play a role in the association of transmembrane proteins with raft membranes. The presence of membrane lipid rafts is suggested in *Giardia* by the observation of the presence of lipid raft-associated molecules including the invariant glycosylphosphatidylinositol (GPI)-anchored surface protein GP49 (Das *et al*., 1991), which alters electrolyte fluxes in cultured human colonic

epithelial T84 cells (Das *et al*., 1994), and palmitoylated and/or myristoylated giardins (Jenkins *et al*., 2009; Saric *et al*., 2009) that could contribute to the attachment of *G. lamblia* trophozoites to the intestinal epithelium (Weiland *et al*., 2005). Moreover, many variant-specific surface proteins (VSPs) that cover the entire surface of *Giardia*, and which are antigenically modified when *Giardia* undergoes antigenic variation are thought to play an important role for evading the host's immune system (Nash, 2001), are palmitoylated (Papanastasiou *et al*., 1997; Hiltpold *et al*., 2000; Touz *et al*., 2005). GP49, an invariant protein, has been identified in strain WB/C6 (Das *et al*., 1991) and palmitoylated variant surface protein H7 in strain GS/H7 (Touz *et al*., 2005). Delta-giardin has been identified in the ventral disk of ATCC strain 30957 WB (Jenkins *et al*., 2009), palmitoylated and myristoylated α-19 giardin in the ventral flagella of the WB/C6 strain (Saric *et al*., 2009), and alpha8-giardin on the plasma membrane and flagella, but not on the ventral disk (Wei *et al*., 2010). It is interesting to note that, as we found here for *G. intestinalis*, disruption of raft-like membrane domains in *E. histolytica* by the cholesterol-binding agents, filipin and MBCD results in the inhibition of several important virulence functions, fluid-phase pinocytosis and adhesion to host cell monolayers (Laughlin *et al*., 2004). A raft-resident adhesin, galactose/*N*-acetylgalactosamine-inhibitable lectin, has been found to be involved in the interaction of *E. histolytica* with the host extracellular matrix by binding to the galactose or *N*-acetylgalactosamine moieties of collagen receptor (Laughlin *et al*., 2004; Mittal *et al*., 2008). Pre-treatment of *G. lamblia* trophozoites with anti-delta-giardin sera caused morphological changes in the parasite and inhibited trophozoite binding to the surface of cell culture slides (Jenkins *et al*., 2009). Since the strong attachment of *G. intestinalis* trophozoites is produced by the adhesive disk and flagella (Müller and von Allmen, 2005; Ankarklev *et al*., 2010), it remains to be determined which lipid raft-associated VSPs and/or giardins associated with ventral disk and/or flagella trigger the lipid raft-dependent adhesion of *G. intestinalis* strains GS/H7, WB/C6 or WB/1267 to human enterocyte-like Caco-2/TC7 cells.

Electron microscopy studies indicate that the close adhesion of *G. intestinalis* trophozoites to intestinal cells by means of their ventral disc directly induces cell damage (Chavez *et al*., 1986; Favennec *et al*., 1991; Teoh *et al*., 2000; Sousa *et al*., 2001). Microvillous shortening, villous flattening or atrophy are all hallmarks of giardiasis. It has been reported that infecting intestinal cells by *G. intestinalis* trophozoites disrupts the cytoskeleton network (Chavez *et al*., 1986; Buret *et al*., 1990; 1991; Favennec *et al*., 1991; Scott *et al*., 2000; Teoh *et al*., 2000). Consistently with these findings, we observed a dramatic disorganization of the apical F-actin in enterocyte-like Caco-2/TC7 cells infected with all the *G. intestinalis* strains examined here. It is worth noting that no modification of apical F-actin developed when the cells were exposed to spent culture supernatants of *G. intestinalis* strains GS/H7, WB/C6 or WB/1267 cultures, or when trophozoite adhesion was inhibited by MBCD treatment. This is consistent with the hypothesis that the cytoskeleton damage is directly associated with the adhesion of the parasite to host cells. However, there is a discrepancy between this finding and a previous observation by Teoh *et al*. (2000), indicating that cultured, non-transformed human duodenal epithelial SCBN and enterocyte-like Caco-2 cells infected with spent culture medium of *G. lamblia* strain S2 showed F-actin rearrangements similar to those promoted by live or lysed *G. lamblia*. This discrepancy could be attributable to the fact that we used different strains in our study, and suggests that active molecule(s) are specifically secreted by strain S2.

Giardia-induced intestinal cell abnormalities lead to the impairment of the digestive process, and this in turn promotes malabsorption and diarrhoea. These abnormalities have been observed in animal models and human biopsies. Buret *et al*. (1990) observed that mice infected with *Giardia muris* developed atrophied intestinal villi and reduced disaccharidase activity. Humen *et al*. (2005), using a gerbil model infected with *G. intestinalis*, have reported the same effect. Interestingly, Daniels and Belosevic (1992; 1995) have reported that C3H/HeN and C57BL/6 mice infected with *G. muris* displayed reduced activities of intestinal lactase, sucrase, trehalase and maltase. Belosevic *et al*. (1989) found that infecting gerbils with *G. lamblia* caused a dramatic decrease in disaccharidase activity. Buret *et al*. (1991; 1992) have reported that in *G. duodenalis*-infected gerbils, the loss of microvillous border surface area is correlated with the reduction in mucosal sucrase and maltase activities, and with that of the jejunal glucose-stimulated absorption of electrolytes, water, and 3-*O*-methyl-D-glucose. In human duodenal biopsy specimens from patients with chronic giardiasis, Troeger *et al*. (2007) observed that sodium-dependent glucose absorption is impaired and active electrogenic anion secretion is activated. *Giardia*-induced disturbance of intestinal functions has been attributed, in part, to shortening of brush border microvilli. In the present article, results obtained after the inhibition of trophozoite adhesion by pre-treating the trophozoites with MBCD or stabilizing the F-actin cytoskeleton by JAS treatment before infection provide evidence that the change in the distribution of brush border-associated SI, DPP IV hydrolases and GLUT5 transporter, and the decrease in sucrose enzyme activity result from the *G. intestinalis*-induced apical F-actin rearrangements.

Structural lesions of the brush border produced by adhering *G. intestinalis* trophozoites have been explained as resulting from the mechanical-tension extraction of microvilli mediated by suction between the ventral disk of the trophozoite and the epithelial intestinal cells forming the brush border (Müller and von Allmen, 2005; Ankarklev *et al*., 2010). The observation here that, even though *G. intestinalis* had adhered to enterocyte-like Caco-2/TC7 cells at 3 h and 12 h p.i., the cells did not display any change in the distribution in the brush border of F-actin, SI and GLUT5 did not fit well with the presence of mechanical tension lesions at the brush border. We observed that the dramatic structural and functional brush border changes in cells infected with the GS/H7 culture seen at 24 h p.i., but not at 3 h and 12 h p.i. despite the fact that the same levels of *G. intestinalis* GS/H7 trophozoites were found at adhering 3 h, 12 h and 24 h p.i. These findings suggest that *G. intestinalis* produces harmful substances in response to adhesion. Analysis of the interaction between *G. intestinalis* and epithelial intestinal cells by transcriptional profiling of interacting trophozoites using *Giardia* microarrays has shown that a total of 200 transcripts were significantly up- or downregulated as a result of the interaction, lasting up to 18 h p.i. (Ringqvist *et al*., 2011). *Giardia* is known to contain and/or release a variety of harmful substances. A sonicate of *G. lamblia* trophozoites leads to an increase in the transepithelial flux and ZO-1 rearrangement (Buret *et al*., 2002). Proteases (Hare *et al*., 1989; Parenti, 1989) and excreted-secreted substances (Chen *et al*., 1995; Kaur *et al*., 2001; Jimenez *et al*., 2004; Shant *et al*., 2004; Rodriguez-Fuentes *et al*., 2006) have been identified in *G. intestinalis*. Contact between *G. lamblia* and epithelial cells triggers the release of proteases (Rodriguez-Fuentes *et al*., 2006), metabolic enzymes including arginine deiminase, ornithine carbamoyl transferase and enolase, which might facilitate the effective colonization of the human small intestine (Ringqvist *et al*., 2008) and elongation factor 1-alpha (Skarin *et al*., 2011).

The integrity of the intestinal layer of epithelial cells is maintained by intercellular junctional complexes composed of TJs, adherent junctions and desmosomes, whereas gap junctions allow intercellular communication to occur (Schneeberger and Lynch, 2004). TJs, the most apical components of the junctional complex, create a semipermeable diffusion barrier between individual cells that can be regulated. Moreover, TJs constitute a functional limit between apical and basolateral cell membrane domains, and also help to maintain cell polarity. It is worth noting that many pathogenic enteric bacteria target and exploit the TJs in their pathogenic strategies (Berkes *et al*., 2003; Guttman and Finlay, 2008a; O'Hara and Buret, 2008). Many studies have shown that there is an increase in intestinal permeability, and a reduction in TER in giardiasis. Cultured SCBN, Caco-2 and MDCK cell monolayers infected with *G. intestinalis* trophozoites displayed a loss of TER and increased paracellular permeability (Chavez *et al*., 1986; Hardin *et al*., 1997; Teoh *et al*., 2000; Buret *et al*., 2002; Chin *et al*., 2002; Dagci *et al*., 2002). *G. intestinalis* or *G. muris* trophozoites disrupted the distribution of ZO-1, which is delocalized from the TJs to the cytosol in SCBN and Caco-2 cells (Buret *et al*., 2002; Chin *et al*., 2002; Scott *et al*., 2002). In human duodenal biopsy specimens from patients with chronic giardiasis, Troeger *et al*. (2007) have observed moderate down expression of the TJ-associated claudin-1 and -7, but not of occludin and claudin-4, accompanied by a decrease in TER and an increase in paracellular permeability. We show here that *G. intestinalis* promotes the phosphorylation of occludin. Phosphorylation events have been reported in enterocytes infected with *G. intestinalis* sonicates, where myosin light chain kinase (MLCK) phosphorylates the myosin light chain at the actomyosin ring, thus altering the distribution of F-actin and the ZO-1 (Scott *et al*., 2002). Taking into consideration the fact that F-actin cytoskeleton disruption caused by *G. intestinalis* trophozoites develops in parallel with the delocalization of the structural TJ-associated protein ZO-1 (Teoh *et al*., 2000; Buret *et al*., 2002; Chin *et al*., 2002; Scott *et al*., 2002), it has been suggested that the *Giardia*-induced disruption of TJs results from disorganization of the F-actin cytoskeleton. In the present study we inhibited *G. intestinalis* adhesion with MBCD and demonstrated that the *G. intestinalis*-induced changes in TER and distribution of TJ-associated proteins depend directly on the adhesion of trophozoites to the brush border. Consistent with the role of structural TJ-associated ZO proteins and their connection with the F-actin cytoskeleton (Fanning *et al*., 1998), and the relevance of structural TJ proteins for the establishment and the maintenance of the TER (Gonzalez-Mariscal *et al*., 2000), we report that JAS treatment of Caco-2/TC7 cells results in inhibition of the *G. intestinalis*-induced loss of TER. The association of occludin with the underlying F-actin cytoskeleton occurs via ZO-1 (Furuse *et al*., 1994; Fanning *et al*., 1998). Accordingly, we observe here that stabilization of the F-actin cytoskeleton of Caco-2/TC7 cells by JAS treatment before infection, abrogates the modification of occludin distribution thus indicating that the *G. intestinalis*-induced rearrangement of occludin at TJs, and the *G. intestinalis*-induced disassembly of apical F-actin cytoskeleton are related events. Alteration of the intestinal barrier as a result of the modification of structural ZO proteins and structural/functional occludin has been reported for both bacterial (Peiffer *et al*., 2000a; Simonovic *et al*., 2000; Sakaguchi *et al*., 2002; Guignot *et al*., 2007) and viral (Obert *et al*., 2000;

Beau *et al*., 2007) enterovirulent pathogens infecting cultured human intestinal T84 or Caco-2 cells forming monolayers.

It has previously been reported that a decrease in the distribution of claudins develops in the intestine of patients with chronic giardiasis (Troeger *et al*., 2007). Claudins, which colocalizes with occludin at the cell membrane, form the backbone of the protein filaments in TJs (Anderson and Van Itallie, 2009; Tepass, 2003). There is evidence that enterovirulent bacteria are able to alter the distribution and properties of claudins, and thus to affect the intestinal barrier (Sakaguchi *et al*., 2002; Muza-Moons *et al*., 2004). Here, we report that in *G. intestinalis*-infected Caco-2/TC7 cells, claudin-1 disappeared from the TJs at the cell-to-cell contact points and relocalized to aggregates located in the central regions of the cells. As for occludin, this rearrangement of claudin-1 results directly from the adhesion of trophozoites, since inhibiting the adhesion by pre-treatment with MBCD, abolishes the delocalization of claudin-1. In contrast to that of occludin, we found that the *G. intestinalis*-induced delocalization of claudin-1 from TJs did not depend on the *G. intestinalis*-induced disassembly of apical F-actin cytoskeleton, since JAS treatment did not prevent the formation of claudin-1 aggregates. Aggresomes are cellular structures formed in response to misfolded proteins (Johnston *et al*., 1998). Aggresome-like structures have been observed in *Salmonella enterica* serovar Typhimurium-infected epithelial cells and macrophages with dramatic remodelling of the networks of cytoplasmic intermediate filament proteins, vimentin and cytokeratin (Guignot and Servin, 2008), and aggresome-like structures in Herpes simplex virus-2-infected Vero cells (Nozawa *et al*., 2004). It remains to be determined: (i) whether *G. intestinalis*-induced claudin-1 aggregates are aggresomes or not, and (ii) whether other claudins are delocalized or not in response to *G. intestinalis* infection.

To summarize, our results show that the adhesion of *G. intestinalis* trophozoites to cultured human enterocyte-like Caco-2/TC7 cells promotes the profound disassembly of the brush border-associated F-actin cell cytoskeleton that in turn leads to a dramatic modification of the distribution of several intestinal brush border-associated enzymes and transporters. In addition, adhesion- and cytoskeleton-dependent changes in TER and occludin distribution are observed in *G. intestinalis*-infected enterocyte-like cells, whereas the change in claudin-1 distribution was adhesion-dependent but cytoskeleton-independent. Similar losses of intestinal microvilli, cytoskeleton-dependent alterations in the distribution and activity of brush border-associated functional proteins, and disruption of epithelial TJs have been observed triggered by bacterial enterovirulent pathogens including attaching-effacing enterohaemorrhagic or enteropathogenic *E. coli* and diffusely adhering *E. coli*, and *Shigella flexneri* (Guttman and Finlay, 2008b). Our *in vitro* observations do not rule out that structural or functional lesions at the brush border of enterocytes can take place *in vivo* following an immune response against *G. intestinalis* infection or the development of cellular caspase-dependent apoptosis as reported by elsewhere (Müller and von Allmen, 2005; Buret, 2007; 2008).

Experimental procedures

Reagents and antibodies

The anti-protease cocktail (leupeptin, aprotinin, antipain, benzamidine, pepstatin A, PMSF), Triton X-100, glucose oxidase-peroxidase reagent and 4-aminoantipyrine were purchased from Sigma Chemicals (Sigma-Aldrich Chimie SARL, L'Isle d'Abeau Chesnes, France). JAS and fluorescein-labelled phalloidin were from Molecular Probes (Junction City, OR). The monoclonal antibodies (mAbs), anti-human sucrase-isomaltase (SI) (8A9) and anti-DPP IV (4H3) were a gift from S. Maroux (ESA 6033 CNRS, Marseille, France). The rabbit polyclonal antibody directed against the fructose transporter GLUT5 was kindly provided by E. Brot-Laroche (Inserm UMR 505, Paris, France). The mAb anti-occludin antibody (clone OC-3F10) and anti-claudin-1 (clone MH25) were supplied by Zymed (Invitrogen, Cergy, France). Secondary fluorescein isothiocyanate (FITC)- or (RITC)-labelled antibodies were from Jackson Immunoresearch Laboratories (Newmarket, England). All other reagents were obtained from Sigma-Aldrich Chimie SARL.

Culture of trophozoites

Giardia intestinalis strain GS/H7 (ATCC 50581) was purchased from the American Type Culture Collection. Clones 1267 and C6 of the WB strain of *G. intestinalis* were kindly provided by Hugo Luján (University of Córdoba, Argentina). Trophozoites were grown in Keister's modified TYI-S-33 medium (Keister, 1983) supplemented with 15 ml per litre of a solution containing 1000 IU ml^{-1} penicillin and 1000 g ml^{-1} streptomycin (Gibco-BRL/Life Technologies, Cergy, France). pH of cultures was adjusted to 6.9 before filter sterilization (0.22 μm). Parasites were cultured in 25 cm^2 cell culture flasks, and harvested as previously described (Perez *et al*., 2001).

Cell culture

The Caco-2/TC7 clone (Chantret *et al*., 1994), established from the parental human enterocyte-like Caco-2 cell line (Fogh *et al*., 1979), was routinely grown in Dulbecco's modified Eagle's minimum essential medium (DMEM) (Invitrogen) with 25 mM glucose (Invitrogen), supplemented with 20% (v/v) heat-inactivated (30 min at 56°C) fetal cal serum (FCS) (Life Technologies) and 1% (v/v) non-essential amino acids (Invitrogen, Cergy, France). Cells were maintained by performing weekly passages using 0.02% trypsin in $Ca^{2+}Mg^{2+}$-free PBS containing 3 mM EDTA to detach cells. Experiments and cell maintenance were carried out at 37°C in a 10% CO_2-90% air atmosphere, and the culture

medium was changed daily. Confluent and fully differentiated cells (cultured for 14 days) were used (Pinto *et al.*, 1983).

Treatments

Jasplakinolide (1 μM) was added to the culture medium of the Caco-2/TC7 cells 30 min before trophozoite infection and maintained during the infection (Peiffer *et al.*, 2001). At the concentrations used, JAS and MBCD did not affect the integrity or viability of the Caco-2/TC7 cells (not shown). In order to investigate the role of lipid rafts in the co-culture of trophozoites and Caco-2/TC7 cells, the cells were pre-treated with MBCD (10 mM) 1 h before trophozoite infection, and MBCD was maintained throughout the 3 h infection period. In order to investigate the role of the lipid rafts of Caco-2/TC7 cells, the cells were pre-treated with MBCD (10 mM) 1 h before trophozoite infection, washed twice with DMEM and then infected. In order to investigate the role of the lipid rafts of *G. intestinalis*, the trophozoites were pre-treated with MBCD (10 mM) for 1 h and washed twice with PBS before being infected. There were no changes in the morphology, motility or proliferation of the trophozoites after MBCD treatment (not shown).

Attachment assay

The attachment assay was carried out as previously described (Sousa *et al.*, 2001). Postconfluence cell monolayers were washed twice with sterile PBS before being infected. Cultures of *G. intestinalis* trophozoites were decanted, and any remaining attached trophozoites were detached by chilling for 10 min in ice-cold PBS, at pH 7.2. Trophozoite suspensions were centrifuged at 1000 *g* for 10 min. The supernatant was discarded, and the pellet was washed once with ice-cold PBS. The pellet was then suspended in DMEM without fetal calf serum (DMEM-adhesion medium). Trophozoite counts were done using a haemocytometer. Suspensions of trophozoites, containing 5×10^5, 1×10^6, 2×10^6 or 8×10^6 trophozoites ml^{-1} (moi 0.5, 1, 2 and 8 respectively), were then co-incubated with cultured cells. Plates were incubated at 37°C in a 10% CO_2-90% air atmosphere. After incubating for 3 h, unattached trophozoites were removed by gently rinsing the culture plates three times with DMEM-adhesion medium at 37°C. Adhering trophozoites were then recovered by incubating at 4°C for 10 min in cold DMEM-adhesion medium. Trophozoite suspensions were counted in a haemocytometer. Assays were conducted in triplicate, with three successive passages of Caco-2/TC7 cells.

Measurement of cell integrity

Cell detachment, necrosis and the release of LDH activity were assessed as reported elsewhere (Minnaard *et al.*, 2001) to evaluate cell integrity and viability.

Measurement of TER

Monolayers of Caco-2/TC7 cells were grown on filters (0.4 μm polyester, tissue culture-treated, Transwell Costar). After apical infection, the integrity of the confluent polarized monolayer was assessed by measuring the TER with a volt-ohmmeter (Millicell-ERS; Millipore, Saint Quentin, France). The background reading for a control filter was subtracted, and results were expressed as percentages of the value for uninfected control cells.

Immunofluorescence

Labelling was conducted as previously reported (Peiffer *et al.*, 2000b) on cells cultured on round glass coverslips (Karl Hecht, 97647 Sondheim, Germany). Briefly, infected cells were washed twice with PBS buffer and fixed for 15 min at room temperature in PBS-3% (w/v) in paraformaldehyde. Monolayers were washed three times with PBS, and then exposed to 50 mM NH_4Cl for 10 min. For cell permeabilization, the coverslips were incubated for 4 min with PBS-0.2% Triton X-100. F-actin labelling was carried out by incubating with FITC-phalloidin (Molecular Probes, Eugene, OR) for 45 min at room temperature. Indirect immunofluorescence labelling of fixed cells was conducted for brush border-associated enzymes (SI, DPPIV and GLUT5), for the transferrin receptor, TJ proteins (occludin and claudin-1) and the adherens junction protein (E-cadherin). Anti-SI, anti-DPPIV and anti-claudin-1 antibodies were diluted 1:50. The anti-GLUT5 antibody was diluted 1:100. Anti-Rc transferin and anti-occludin antibodies were diluted 1:100; and the anti-E-cadherin antibody was diluted 1:300. All dilutions were performed in 0.2% (v/v) gelatin-PBS. The cells were incubated for 45 min at room temperature with the primary antibody. After three washes with PBS, the cells were incubated for another 45 min in the dark and at room temperature with the secondary antibody conjugated with FITC or TRITC diluted 1:200 in 0.2% gelatin-PBS. After exhaustive washing, samples were mounted in DakoCytomation fluorescent mounting medium for immunofluorescence examination. The coverslips were examined by conventional epifluorescence microscopy using a Leitz Aristoplan microscope. No fluorescence was detected when the primary antibody was omitted. Confocal analysis was performed using a CLMS (model LSM 510 Zeiss, equipped with an air-cooled, 488 nm argon ion laser, and a 543 nm helium neon laser) configured with an Axiovert 100M microscope using a Plan Apochromat 63 ×/1.40 oil objective. Images obtained by CLMS were analysed using Imaris software (version 6.21) (Bitplane, Zurich).

Preparation of Triton-soluble and Triton-resistant fractions

After infection, the cells were washed once with cold PBS, and treated with 700 μl of Triton extraction buffer (Hepes 25 mM, Triton X-100 0.5%, NaCl 150 mM, EDTA 2 mM, protease inhibitors: phenyl-methylsulfonyl fluoride, aprotinin 10 μg ml^{-1}, leupeptin 10 μg ml^{-1}, pepstatin 10 μg ml^{-1}, sodium orthovanadate 4 mM, NaF 40 mM) for 10 min at 4°C. Cell supernatants were collected by centrifuging (Triton-soluble fraction). The cells were treated with 465 μl of Laemmli buffer plus iodoacetamide and 700 μl of Triton X-100 extraction buffer (Triton-resistant fraction). Both fractions were resolved in 10% SDS-PAGE gels and analysed by Western blot.

Western blot analysis

SDS-PAGE gels were transferred onto a PVDF membrane (Immobilon-P; Millipore). Mouse anti-occludin (1/500) and rabbit

anti-claudin-1 (1/250) antibodies were used to detect the TJ proteins. A secondary anti-rabbit or anti-mouse horseradish peroxidase-conjugated antibody was also used. A chemiluminescence analysis was then performed (ECL system Millipore). Quantification was carried out using the Scion Image processor software.

Enzyme assay

The cells were washed in ice-cold PBS, scraped off, suspended in PBS and homogenized. Sucrase activity was measured in the enriched brush border membrane fraction obtained after centrifuging the cell homogenates for 1 h at 100 000 *g* and at 4°C as previously described (Peiffer *et al*., 2001). Briefly, sucrase activity was assayed using a glucose oxidase/peroxidase reagent that contains 4-amino-antipyrine. Sucrase activity was determined by measuring the amount of glucose liberated from the sucrose. One unit is defined as the amount of enzyme that hydrolyses 1 μM of substrate min^{-1} at 37°C. Enzyme-specific activity is expressed as milliunits (mU) per mg of protein. Proteins were determined by the BCA assay.

Statistical analysis

All experiments were conducted in triplicate. The results are expressed as the mean ± standard deviation of the mean (SD). Student's *t*-test was used for statistical comparisons.

Acknowledgements

We are grateful to Alain L. Servin (Inserm U756) for his continuous support and critical analysis of the manuscript. We are also indebted to Raymonde Amsellem (Inserm U756) for technical assistance with cell cultures. We would also like to thank V. Nicolas (Plateforme d'Imagerie Cellulaire. IFR141. Faculté de Pharmacie Châtenay-Malabry) for expert assistance with confocal laser scanning microscopy.

This work was funded by institutional French fundings: the Institut National de la Santé et de la Recherche Médicale (Inserm), Université Paris-Sud 11 and Ministère de la Recherche (UMR 756).

M.A.H. was supported by the Programme AlBan, the European Union Programme of High Level Scholarships for Latin America, scholarship N° E07D402549AR. M.A.H. is a fellow at the Consejo Nacional de Investigaciones Científicas y Técnicas (CONICET), Argentina. P.F.P. is a member of the Carrera del Investigador Científico y Tecnológico of the CONICET, Argentina.

References

Anderson, J.M., and Van Itallie, C.M. (2009) Physiology and function of the tight junction. *Cold Spring Harb Perspect Biol* **1:** a002584.

Ankarklev, J., Jerlstrom-Hultqvist, J., Ringqvist, E., Troell, K., and Svard, S.G. (2010) Behind the smile: cell biology and disease mechanisms of *Giardia* species. *Nat Rev Microbiol* **8:** 413–422.

Beau, I., Cotte-Laffitte, J., Amsellem, R., and Servin, A.L. (2007) A protein kinase A-dependent mechanism by which rotavirus affects the distribution and mRNA level of the functional tight junction-associated protein, occludin, in human differentiated intestinal Caco-2 cells. *J Virol* **81:** 8579–8586.

Belosevic, M., Faubert, G.M., and MacLean, J.D. (1989) Disaccharidase activity in the small intestine of gerbils (*Meriones unguiculatus*) during primary and challenge infections with *Giardia lamblia*. *Gut* **30:** 1213–1219.

Berkes, J., Viswanathan, V.K., Savkovic, S.D., and Hecht, G. (2003) Intestinal epithelial responses to enteric pathogens: effects on the tight junction barrier, ion transport, and inflammation. *Gut* **52:** 439–451.

Bernander, R., Palm, J.E., and Svard, S.G. (2001) Genome ploidy in different stages of the *Giardia lamblia* life cycle. *Cell Microbiol* **3:** 55–62.

Boyle, E.C., and Finlay, B.B. (2003) Bacterial pathogenesis: exploiting cellular adherence. *Curr Opin Cell Biol* **15:** 633–639.

Buret, A.G. (2007) Mechanisms of epithelial dysfunction in giardiasis. *Gut* **56:** 316–317.

Buret, A.G. (2008) Pathophysiology of enteric infections with *Giardia duodenalis*. *Parasite* **15:** 261–265.

Buret, A., Gall, D.G., and Olson, M.E. (1990) Effects of murine giardiasis on growth, intestinal morphology, and disaccharidase activity. *J Parasitol* **76:** 403–409.

Buret, A., Gall, D.G., and Olson, M.E. (1991) Growth, activities of enzymes in the small intestine, and ultrastructure of microvillous border in gerbils infected with *Giardia duodenalis*. *Parasitol Res* **77:** 109–114.

Buret, A., Hardin, J.A., Olson, M.E., and Gall, D.G. (1992) Pathophysiology of small intestinal malabsorption in gerbils infected with *Giardia lamblia*. *Gastroenterology* **103:** 506–513.

Buret, A.G., Mitchell, K., Muench, D.G., and Scott, K.G. (2002) *Giardia lamblia* disrupts tight junctional ZO-1 and increases permeability in non-transformed human small intestinal epithelial monolayers: effects of epidermal growth factor. *Parasitology* **125:** 11–19.

Cevallos, A., Carnaby, S., James, M., and Farthing, J.G. (1995) Small intestinal injury in a neonatal rat model of giardiasis is strain dependent. *Gastroenterology* **109:** 766–773.

Chantret, I., Rodolosse, A., Barbat, A., Dussaulx, E., Brot-Laroche, E., Zweibaum, A., and Rousset, M. (1994) Differential expression of sucrase-isomaltase in clones isolated from early and late passages of the cell line Caco-2: evidence for glucose-dependent negative regulation. *J Cell Sci* **107:** 213–225.

Chavez, B., Knaippe, F., Gonzalez-Mariscal, L., and Martinez-Palomo, A. (1986) *Giardia lamblia*: electrophysiology and ultrastructure of cytopathology in cultured epithelial cells. *Exp Parasitol* **61:** 379–389.

Chen, N., Upcroft, J.A., and Upcroft, P. (1995) A *Giardia duodenalis* gene encoding a protein with multiple repeats of a toxin homologue. *Parasitology* **111:** 423–431.

Chin, A.C., Teoh, D.A., Scott, K.G., Meddings, J.B., Macnaughton, W.K., and Buret, A.G. (2002) Strain-dependent induction of enterocyte apoptosis by *Giardia lamblia* disrupts epithelial barrier function in a caspase-3-dependent manner. *Infect Immun* **70:** 3673–3680.

Dagci, H., Ustun, S., Taner, M.S., Ersoz, G., Karacasu, F., and Budak, S. (2002) Protozoon infections and intestinal permeability. *Acta Trop* **81:** 1–5.

Daniels, C.W., and Belosevic, M. (1992) Disaccharidase activity in the small intestine of susceptible and resistant mice after primary and challenge infections with *Giardia muris*. *Am J Trop Med Hyg* **46:** 382–390.

Daniels, C.W., and Belosevic, M. (1995) Disaccharidase activity in male and female C57BL/6 mice infected with *Giardia muris*. *Parasitol Res* **81:** 143–147.

Das, S., Traynor-Kaplan, A., Reiner, D.S., Meng, T.C., and Gillin, F.D. (1991) A surface antigen of *Giardia lamblia* with a glycosylphosphatidylinositol anchor. *J Biol Chem* **266:** 21318–21325.

Das, S., Traynor-Kaplan, A., Kachintorn, U., Aley, S.B., and Gillin, F.D. (1994) GP49, an invariant GPI-anchored antigen of *Giardia lamblia*. *Braz J Med Biol Res* **27:** 463–469.

Fanning, A.S., Jameson, B.J., Jesaitis, L.A., and Anderson, J.M. (1998) The tight junction protein ZO-1 establishes a link between the transmembrane protein occludin and the actin cytoskeleton. *J Biol Chem* **273:** 29745–29753.

Farshori, P., and Kachar, B. (1999) Redistribution and phosphorylation of occludin during opening and resealing of tight junctions in cultured epithelial cells. *J Membr Biol* **170:** 147–156.

Favennec, L., Magne, D., and Gobert, J.G. (1991) Cytopathogenic effect of *Giardia intestinalis, in vitro*. *Parasitol Today* **7:** 141.

Fogh, J., Orfeo, T., Tiso, J., and Sharkey, F.E. (1979) Establishment of human colon carcinoma lines in nude mice. *Exp Cell Biol* **47:** 136–144.

Furuse, M., Hirase, T., Itoh, M., Nagafuchi, A., Yonemura, S., and Tsukita, S. (1993) Occludin: a novel integral membrane protein localizing at tight junctions. *J Cell Biol* **123:** 1777–1788.

Furuse, M., Itoh, M., Hirase, T., Nagafuchi, A., Yonemura, S., Tsukita, S., and Tsukita, S. (1994) Direct association of occludin with ZO-1 and its possible involvement in the localization of occludin at tight junctions. *J Cell Biol* **127:** 1617–1626.

Furuse, M., Fujita, K., Hiiragi, T., Fujimoto, K., and Tsukita, S. (1998) Claudin-1 and -2: novel integral membrane proteins localizing at tight junctions with no sequence similarity to occludin. *J Cell Biol* **141:** 1539–1550.

Gonzalez-Mariscal, L., Betanzos, A., and Avila-Flores, A. (2000) MAGUK proteins: structure and role in the tight junction. *Semin Cell Dev Biol* **11:** 315–324.

van der Goot, F.G., and Harder, T. (2001) Raft membrane domains: from a liquid-ordered membrane phase to a site of pathogen attack. *Semin Immunol* **13:** 89–97.

Gorowara, S., Ganguly, N.K., Mahajan, R.C., and Walia, B.N. (1992) Study on the mechanism of *Giardia lamblia* induced diarrhoea in mice. *Biochim Biophys Acta* **1138:** 122–126.

Guignot, J., and Servin, A.L. (2008) Maintenance of the *Salmonella*-containing vacuole in the juxtanuclear area: a role for intermediate filaments. *Microb Pathog* **45:** 415–422.

Guignot, J., Chaplais, C., Coconnier-Polter, M.H., and Servin, A.L. (2007) The secreted autotransporter toxin, Sat, functions as a virulence factor in Afa/Dr diffusely adhering *Escherichia coli* by promoting lesions in tight junction of polarized epithelial cells. *Cell Microbiol* **9:** 204–221.

Guttman, J.A., and Finlay, B.B. (2008a) Tight junctions as targets of infectious agents. *Biochim Biophys Acta* **1788:** 832–841.

Guttman, J.A., and Finlay, B.B. (2008b) Subcellular alterations that lead to diarrhea during bacterial pathogenesis. *Trends Microbiol* **16:** 535–542.

Hardin, J.A., Buret, A.G., Olson, M.E., Kimm, M.H., and Gall, D.G. (1997) Mast cell hyperplasia and increased macromolecular uptake in an animal model of giardiasis. *J Parasitol* **83:** 908–912.

Hare, D.F., Jarroll, E.L., and Lindmark, D.G. (1989) *Giardia lamblia*: characterization of proteinase activity in trophozoites. *Exp Parasitol* **68:** 168–175.

Hiltpold, A., Frey, M., Hulsmeier, A., and Kohler, P. (2000) Glycosylation and palmitoylation are common modifications of *Giardia* variant surface proteins. *Mol Biochem Parasitol* **109:** 61–65.

Humen, M.A., De Antoni, G.L., Benyacoub, J., Costas, M.E., Cardozo, M.I., Kozubsky, L., *et al*. (2005) *Lactobacillus johnsonii* La1 antagonizes *Giardia intestinalis in vivo*. *Infect Immun* **73:** 1265–1269.

Jenkins, M.C., O'Brien, C.N., Murphy, C., Schwarz, R., Miska, K., Rosenthal, B., and Trout, J.M. (2009) Antibodies to the ventral disc protein delta-giardin prevent *in vitro* binding of *Giardia lamblia* trophozoites. *J Parasitol* **95:** 895–899.

Jimenez, J.C., Fontaine, J., Grzych, J.M., Dei-Cas, E., and Capron, M. (2004) Systemic and mucosal responses to oral administration of excretory and secretory antigens from *Giardia intestinalis*. *Clin Diagn Lab Immunol* **11:** 152–160.

Johnston, J.A., Ward, C.L., and Kopito, R.R. (1998) Aggresomes: a cellular response to misfolded proteins. *J Cell Biol* **143:** 1883–1898.

Jung, H.C., Eckmann, L., Yang, S.K., Panja, A., Fierer, J., Morzycka-Wroblewska, E., and Kagnoff, M.F. (1995) A distinct array of proinflammatory cytokines is expressed in human colon epithelial cells in response to bacterial invasion. *J Clin Invest* **95:** 55–65.

Kamda, J.D., and Singer, S.M. (2009) Phosphoinositide 3-kinase-dependent inhibition of dendritic cell interleukin-12 production by *Giardia lamblia*. *Infect Immun* **77:** 685–693.

Katelaris, P.H., Naeem, A., and Farthing, M.J. (1995) Attachment of *Giardia lamblia* trophozoites to a cultured human intestinal cell line. *Gut* **37:** 512–518.

Kaur, H., Ghosh, S., Samra, H., Vinayak, V.K., and Ganguly, N.K. (2001) Identification and characterization of an excretory-secretory product from *Giardia lamblia*. *Parasitology* **123:** 347–356.

Keister, D.B. (1983) Axenic culture of *Giardia lamblia* in TYI-S-33 medium supplemented with bile. *Trans R Soc Trop Med Hyg* **77:** 487–488.

Lambert, D., O'Neill, C.A., and Padfield, P.J. (2007) Methyl-beta-cyclodextrin increases permeability of Caco-2 cell monolayers by displacing specific claudins from cholesterol rich domains associated with tight junctions. *Cell Physiol Biochem* **20:** 495–506.

Laughlin, R.C., McGugan, G.C., Powell, R.R., Welter, B.H., and Temesvari, L.A. (2004) Involvement of raft-like plasma membrane domains of *Entamoeba histolytica* in pinocytosis and adhesion. *Infect Immun* **72:** 5349–5357.

Lencer, W.I. (2001) Microbial invasion across the intestinal epithelial barrier. *Pediatr Res* **49:** 4–5.

Lievin-Le Moal, V., and Servin, A.L. (2006) The front line of enteric host defense against unwelcome intrusion of harmful microorganisms: mucins, antimicrobial peptides, and microbiota. *Clin Microbiol Rev* **19:** 315–337.

Lujan, H.D. (2006) *Giardia* and giardiasis. *Medicina (B Aires)* **66:** 70–74.

Minnaard, J., Humen, M., and Perez, P.F. (2001) Effect of *Bacillus cereus* exocellular factors on human intestinal epithelial cells. *J Food Prot* **64:** 1535–1541.

Mittal, K., Welter, B.H., and Temesvari, L.A. (2008) *Entamoeba histolytica*: lipid rafts are involved in adhesion of trophozoites to host extracellular matrix components. *Exp Parasitol* **120:** 127–134.

Monajemzadeh, S.M., and Monajemzadeh, M. (2008) Comparison of iron and hematological indices in *Giardia lamblia* infection before and after treatment in 102 children in Ahwaz, Iran. *Med Sci Monit* **14:** CR19–CR23.

Müller, N., and von Allmen, N. (2005) Recent insights into the mucosal reactions associated with *Giardia lamblia* infections. *Int J Parasitol* **35:** 1339–1347.

Muza-Moons, M.M., Schneeberger, E.E., and Hecht, G.A. (2004) Enteropathogenic *Escherichia coli* infection leads to appearance of aberrant tight junctions strands in the lateral membrane of intestinal epithelial cells. *Cell Microbiol* **6:** 783–793.

Nash, T.E., Lujan, H.T., Mowatt, M.R., and Conrad, J.T. (2001) Variant-specific surface protein switching in *Giardia lamblia*. *Infect Immun* **69:** 1922–1923.

Nozawa, N., Yamauchi, Y., Ohtsuka, K., Kawaguchi, Y., and Nishiyama, Y. (2004) Formation of aggresome-like structures in herpes simplex virus type 2-infected cells and a potential role in virus assembly. *Exp Cell Res* **299:** 486–497.

Oberhuber, G., Kastner, N., and Stolte, M. (1997) Giardiasis: a histologic analysis of 567 cases. *Scand J Gastroenterol* **32:** 48–51.

Obert, G., Peiffer, I., and Servin, A.L. (2000) Rotavirus-induced structural and functional alterations in tight junctions of polarized intestinal Caco-2 cell monolayers. *J Virol* **74:** 4645–4651.

O'Hara, J.R., and Buret, A.G. (2008) Mechanisms of intestinal tight junctional disruption during infection. *Front Biosci* **13:** 7008–7021.

Palm, D., Weiland, M., McArthur, A.G., Winiecka-Krusnell, J., Cipriano, M.J., Birkeland, S.R., *et al*. (2005) Developmental changes in the adhesive disk during *Giardia* differentiation. *Mol Biochem Parasitol* **141:** 199–207.

Papanastasiou, P., McConville, M.J., Ralton, J., and Kohler, P. (1997) The variant-specific surface protein of *Giardia*, VSP4A1, is a glycosylated and palmitoylated protein. *Biochem J* **322:** 49–56.

Parenti, D.M. (1989) Characterization of a thiol proteinase in *Giardia lamblia*. *J Infect Dis* **160:** 1076–1080.

Pegado, M.G., and de Souza, W. (1994) Role of surface components in the process of interaction of *Giardia duodenalis* with epithelial cells *in vitro*. *Parasitol Res* **80:** 320–326.

Peiffer, I., Blanc-Potard, A.B., Bernet-Camard, M.F., Guignot, J., Barbat, A., and Servin, A.L. (2000a) Afa/Dr diffusely adhering *Escherichia coli* C1845 infection promotes selective injuries in the junctional domain of polarized human intestinal Caco-2/TC7 cells. *Infect Immun* **68:** 3431–3442.

Peiffer, I., Guignot, J., Barbat, A., Carnoy, C., Moseley, S.L., Nowicki, B.J., *et al*. (2000b) Structural and functional lesions in brush border of human polarized intestinal Caco-2/TC7 cells infected by members of the Afa/Dr diffusely adhering family of *Escherichia coli*. *Infect Immun* **68:** 5979–5990.

Peiffer, I., Bernet-Camard, M.F., Rousset, M., and Servin, A.L. (2001) Impairments in enzyme activity and biosynthesis of brush border-associated hydrolases in human intestinal Caco-2/TC7 cells infected by members of the Afa/Dr family of diffusely adhering *Escherichia coli*. *Cell Microbiol* **3:** 341–357.

Perez, P.F., Minnaard, J., Rouvet, M., Knabenhans, C., Brassart, D., De Antoni, G.L., and Schiffrin, E.J. (2001) Inhibition of *Giardia intestinalis* by extracellular factors from lactobacilli: an *in vitro* study. *Appl Environ Microbiol* **67:** 5037–5042.

Peterson, M.D., and Mooseker, M.S. (1992) Characterization of the enterocyte-like brush border cytoskeleton of the C2BBe clones of the human intestinal cell line, Caco-2. *J Cell Sci* **102:** 581–600.

Peterson, M.D., and Mooseker, M.S. (1993) An *in vitro* model for the analysis of intestinal brush border assembly. I. Ultrastructural analysis of cell contact-induced brush border assembly in Caco-2BBe cells. *J Cell Sci* **105:** 445–460.

Peterson, M.D., Bement, W.M., and Mooseker, M.S. (1993) An *in vitro* model for the analysis of intestinal brush border assembly. II. Changes in expression and localization of brush border proteins during cell contact-induced brush border assembly in Caco-2BBe cells. *J Cell Sci* **105:** 461–472.

Pinto, M., Robine-Leon, S., Appay, M.D., Kedinger, M., Triadou, N., Dussaulx, E., *et al*. (1983) Enterocyte-like differentiation and polarization of the human colon carcinoma cell line Caco-2 in culture. *Biol Cell* **47:** 323–330.

Ringqvist, E., Palm, J.E., Skarin, H., Hehl, A.B., Weiland, M., Davids, B.J., *et al*. (2008) Release of metabolic enzymes by *Giardia* in response to interaction with intestinal epithelial cells. *Mol Biochem Parasitol* **159:** 85–91.

Ringqvist, E., Avesson, L., Soderbom, F., and Svard, S.G. (2011) Transcriptional changes in *Giardia* during host–parasite interactions. *Int J Parasitol* **41:** 277–285.

Rodriguez-Fuentes, G.B., Cedillo-Rivera, R., Fonseca-Linan, R., Arguello-Garcia, R., Munoz, O., Ortega-Pierres, G., and Yepez-Mulia, L. (2006) *Giardia duodenalis*: analysis of secreted proteases upon trophozoite-epithelial cell interaction *in vitro*. *Mem Inst Oswaldo Cruz* **101:** 693–696.

Roxstrom-Lindquist, K., Ringqvist, E., Palm, D., and Svard, S. (2005) *Giardia lamblia*-induced changes in gene expression in differentiated Caco-2 human intestinal epithelial cells. *Infect Immun* **73:** 8204–8208.

Sackey, M.E., Weigel, M.M., and Armijos, R.X. (2003) Predictors and nutritional consequences of intestinal parasitic

infections in rural Ecuadorian children. *J Trop Pediatr* **49:** 17–23.

Sakaguchi, T., Kohler, H., Gu, X., McCormick, B.A., and Reinecker, H.C. (2002) *Shigella flexneri* regulates tight junction-associated proteins in human intestinal epithelial cells. *Cell Microbiol* **4:** 367–381.

Saric, M., Vahrmann, A., Niebur, D., Kluempers, V., Hehl, A.B., and Scholze, H. (2009) Dual acylation accounts for the localization of {alpha}19-giardin in the ventral flagellum pair of *Giardia lamblia*. *Eukaryot Cell* **8:** 1567–1574.

Schneeberger, E.E., and Lynch, R.D. (2004) The tight junction: a multifunctional complex. *Am J Physiol Cell Physiol* **286:** C1213–C1228.

Scott, K.G., Logan, M.R., Klammer, G.M., Teoh, D.A., and Buret, A.G. (2000) Jejunal brush border microvillous alterations in *Giardia* muris-infected mice: role of T lymphocytes and interleukin-6. *Infect Immun* **68:** 3412–3418.

Scott, K.G., Meddings, J.B., Kirk, D.R., Lees-Miller, S.P., and Buret, A.G. (2002) Intestinal infection with *Giardia* spp. reduces epithelial barrier function in a myosin light chain kinase-dependent fashion. *Gastroenterology* **123:** 1179–1190.

Shant, J., Ghosh, S., Bhattacharyya, S., Ganguly, N.K., and Majumdar, S. (2004) The alteration in signal transduction parameters induced by the excretory-secretory product from *Giardia lamblia*. *Parasitology* **129:** 421–430.

Simonovic, I., Rosenberg, J., Koutsouris, A., and Hecht, G. (2000) Enteropathogenic *Escherichia coli* dephosphorylates and dissociates occludin from intestinal epithelial tight junctions. *Cell Microbiol* **2:** 305–315.

Singh, K.D., Bhasin, D.K., Rana, S.V., Vaiphei, K., Katyal, R., Vinayak, V.K., and Singh, K. (2000) Effect of *Giardia lamblia* on duodenal disaccharidase levels in humans. *Trop Gastroenterol* **21:** 174–176.

Skarin, H., Ringqvist, E., Hellman, U., and Svard, S.G. (2011) Elongation factor 1-alpha is released into the culture medium during growth of *Giardia intestinalis* trophozoites. *Exp Parasitol* **127:** 804–810.

Sousa, M.C., Goncalves, C.A., Bairos, V.A., and Poiares-Da-Silva, J. (2001) Adherence of *Giardia lamblia* trophozoites to Int-407 human intestinal cells. *Clin Diagn Lab Immunol* **8:** 258–265.

Teoh, D.A., Kamieniecki, D., Pang, G., and Buret, A.G. (2000) *Giardia lamblia* rearranges F-actin and alpha-actinin in human colonic and duodenal monolayers and reduces transepithelial electrical resistance. *J Parasitol* **86:** 800–806.

Tepass, U. (2003) Claudin complexities at the apical junctional complex. *Nat Cell Biol* **5:** 595–597.

Touz, M.C., Conrad, J.T., and Nash, T.E. (2005) A novel palmitoyl acyl transferase controls surface protein palmitoylation and cytotoxicity in *Giardia lamblia*. *Mol Microbiol* **58:** 999–1011.

Troeger, H., Epple, H.J., Schneider, T., Wahnschaffe, U., Ullrich, R., Burchard, G.D., *et al*. (2007) Effect of chronic *Giardia lamblia* infection on epithelial transport and barrier function in human duodenum. *Gut* **56:** 328–335.

Wei, C.J., Tian, X.F., Adam, R.D., and Lu, S.Q. (2010) *Giardia lamblia*: intracellular localization of alpha8-giardin. *Exp Parasitol* **126:** 489–496.

Weiland, M.E., McArthur, A.G., Morrison, H.G., Sogin, M.L., and Svard, S.G. (2005) Annexin-like alpha giardins: a new cytoskeletal gene family in *Giardia lamblia*. *Int J Parasitol* **35:** 617–626.

Zweibaum, A., Laburthe, M., Grasset, E., and Louvard, D. (1991) Use of cultured cell lines in studies of intestinal cell differentiation and function. In *Handbook of Physiology, the Gastrointestinal System, Intestinal Absorption and Secretion*. Schultz, S.J., and Frizell, R.A. (eds). Bethesda: American Physiological Society, pp. 223–255.